R/V ALKOR Cruise Report 512

North Sea Blowouts

15th July – 26th July, 2018

Cuxhaven - Kiel (Germany)

Jens Karstens, Jens Schneider von Deimling, Christoph Böttner, Judith Elger, Helene-Sophie Hilbert, Michel Kühn, Rebecca Kühn, Philipp Müller, Benedict Reinardy, Bettina Schramm

Table of Contents

1 Introduction

Focused fluid flow through marine sediments is primarily controlled by contrasts in permeability and pore pressure and the presence of mobile pore fluids. Most fluids migrate diffusively through the interconnected pore space of marine sediments. The presence of very low or impermeable layers (e.g. mudstones, evaporates, carbonates) may prohibit the equilibration of pore pressure by diffusive flow, which leads to the accumulation of pore overpressure. If the pore overpressure exceeds the caprock's resistance against capillary or fracture failure, the overpressure is released by the formation of strata-crosscutting focused fluid conduits, preferentially through zones of structural weakness (Figure 1; Clayton and Hay, 1994; Berndt, 2005; Cartwright et al., 2007; Løseth et al., 2009).

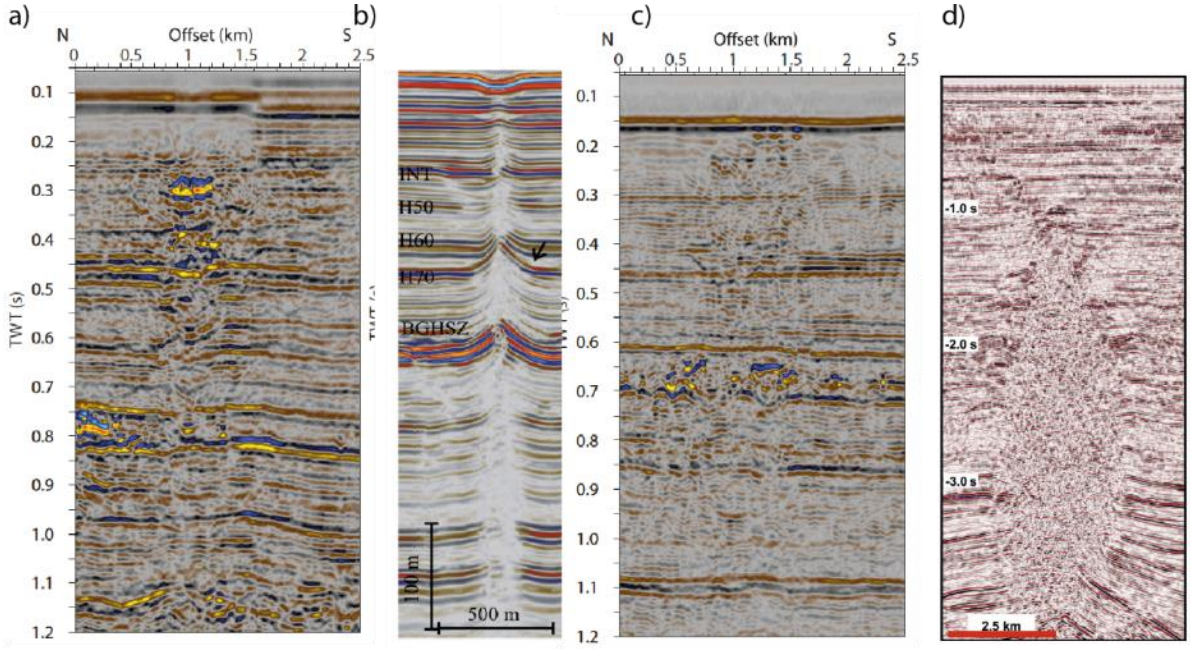

Figure 1: a) Pipe structure from the Southern Viking Graben (Karstens and Berndt, 2015). b) Pipe structure from the Nyegga (Plaza Faverola et al., 2011). c) Chimney structure from the Southern Viking Graben (Karstens and Berndt, 2015). d) Chimney structure at Tommeliten (Løseth et al., 2009).

Focused fluid conduits are often found above hydrocarbon fields in the North Sea (e.g. Tommeliten, Ekofisk; Arntsen et al., 2007; Granli et al., 1999) and can be used as an indicator for hydrocarbon reservoirs (Løseth et al., 2009). Focused fluid conduits are also very important for the long-term efficiency of subsurface storage operations (Karstens et al., 2017). Especially the geological storage of CO_2 as part of Carbon Capture and Storage (CCS) operations may become highly relevant in the future, whereas the North Sea Basin hosts ideal storage formations for the industrial-scale implementation of this technology in Europe. The presence of focused fluid conduits is additionally important for the assessment of drilling hazard associated with shallow, overpressured gas accumulations within the Quaternary succession of the North Sea Basin. Drilling into these reservoirs has resulted in uncontrollable blowout events including the West Vanguard blowout (Norwegian Sea) in 1985 (Judd & Hovland, 2007) and the 22/4B blowout (British North Sea) in 1990 (Leifer and Judd, 2015). These events highlight the importance of understanding shallow fluid flow systems, even when these are not connected with deep hydrocarbon reservoirs.

The North Sea Basin is Europe's most prolific hydrocarbon province and has been explored since the early 1960s. The first-ever offshore North Sea well was drilled in the German Sector of the North Sea in 1964. The exploration well B1 was drilled to a depth of 2925 m, when it broke through an anhydrite layer overlying a gas charged dolomite reservoir (Kornfeld, 1964). The reservoir contained overpressured gas (mainly nitrogen), which cut through the drilling mud into the well string and

initiated a blowout on the 24th of June 1964 (Kornfeld, 1964). The well could be sealed by a blowout preventer and overpressure retained in the well. At dawn of the following day, workers could see vigorous gas release at the sea surface about 400 m away from the drilling rig "Mr. Louie". The overpressured fluid breached the well and created a focused fluid conduit that continued to the seafloor, where gas expulsion created a crater later known as the Figge Maar (Thatje et al., 1999, Judd and Hovland, 2007). The crater is located about 30 nm west of Helgoland and 35 nm north of Juist.

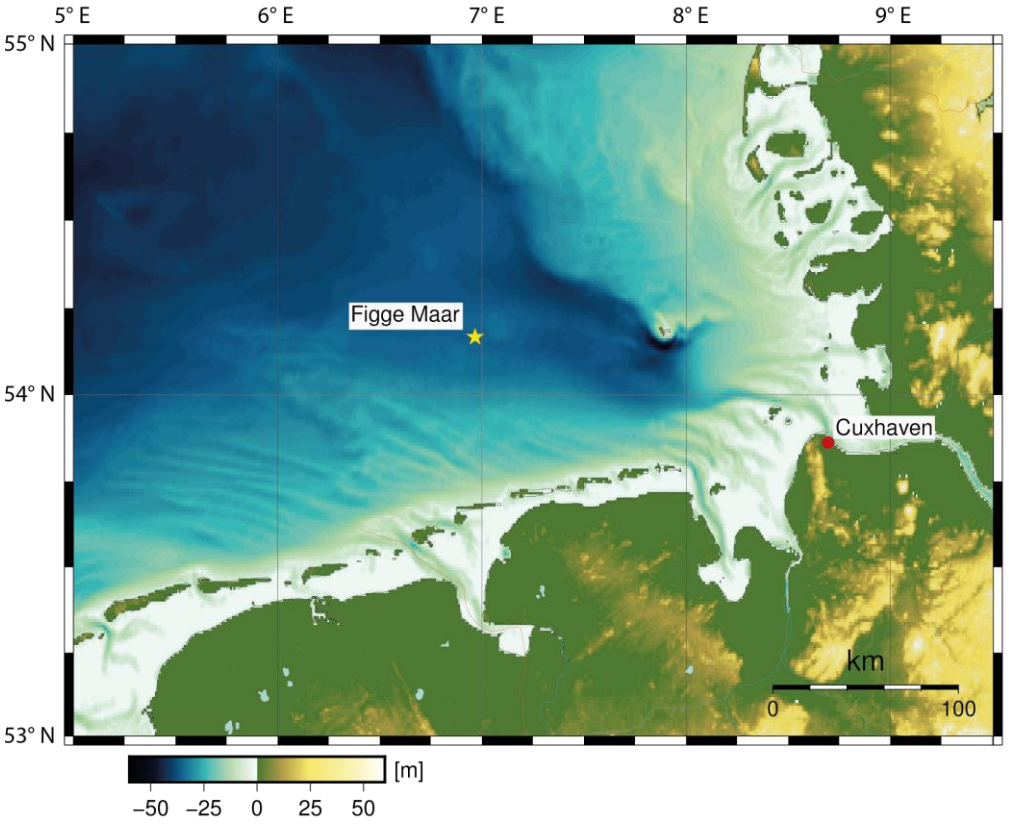

Figure 2: Map of the study area showing the location of the Figge Maar.

Gas escaped vigorously for weeks (according to news reports, e.g. Hamburger Abendblatt, 28.07.64) and the created seafloor crater had an initial depth of 65 m below sea level and a diameter of 400 m (Thatje et al., 1999). A bathymetric survey in 1995 revealed that the depth of the crater has decreased to 50.9 m below sea level (Thatje et al., 1999). The Figge Maar crater has not been surveyed ever since until the Poseidon cruise POS518 in October 2017, which revisited the Figge Maar in preparation of this expedition (Linke & Haeckel, 2018).

The cruise AL512 represents the first-ever geoscientific research campaign surveying the Figge Maar and its main motivation is to image the fluid migration pathways that formed the Figge Maar crater with multi-resolution hydroacoustic and seismic datasets. The investigations will help to understand the evolution and hydraulic properties of focused fluid conduits. The cruise will survey the ongoing methane release from the crater. Furthermore, our experiments will allow reconstructing the temporal and structural evolution of a seafloor depression formed by the rapid expulsion of gas.

2 Narrative of the Cruise

A group of five scientists and technicians boarded R/V ALKOR already in the afternoon of the **13th of July**. The scientific equipment was delivered to the ship in the morning of the **14th of July**. The equipment was unpacked, installed and secured during the day and the rest of the scientific crew arrived in the afternoon to help finalizing the mobilization.

The cruise started on Sunday, **15th of July** at 9:30 from Cuxhaven and R/V ALKOR headed towards the research area, where we arrived in the afternoon. The first experiment of our campaign was the acquisition of 2D reflection seismic profiles using a streamer with 136 channels and an active length of 212.5 m. During the evening and the night, we acquired three seismic profiles crossing the Figge Maar in W-E, NE-SW and S-N direction. During the seismic measurement, we simultaneously acquired sediment echosounder profiles. In the morning of the **16th of July**, we recovered the seismic streamer and the airgun and begun with the deployment of 15 Ocean-Bottom-Seismometer (OBS) within and around the Figge Maar crater. The deployment was finished at 16:00 and we began a 3 nm x 3 nm bathymetry survey using a NORBIT multibeam system. The multibeam bathymetry survey was finished in the morning of the **17th of July**. Afterwards, we deployed the P-Cable system equipped with 12 streamers and the airgun. However, the trigger line of the airgun was malfunctioning and we had to recover the airgun again. At the same time, the control unit of the P-Cable system indicated connection problems and we had to recover the P-Cable as well.

Both technical problems could be solved and we collected some additional multibeam lines for filling up gaps in our grid. Afterwards, we began a flare imaging survey using the shipboard EK60 echosounder. For these surveys, the ship drifted multiple times above the Figge Maar with a speed of 1 knot. In the morning of the **18th of July**, sea conditions did not allow the deployment of the P-Cable system and we started collecting dedicated seismic profiles for the OBS experiment. We acquired three circular profiles and ten linear profiles, which were additionally surveyed with a short streamer consisting of four streamer segments. During nighttime, the bridge of the ALKOR successfully stopped a fish trawler from running over the OBS stations by giving signals with the horn. The acquisition of the OBS profiles was finalized at midday of the **19th of July** and the P-Cable was deployed a second time. After a short duration of surveying, the P-Cable system developed again a technical problem and we had to recover it after 21:00. During the following night, we filled acquisition gaps of the multibeam survey and started a dedicated water column imaging survey to detect flares within and south of the Figge Maar crater, which was finished at midday of the **20th of July**.

Afterwards, we deployed the airgun and a streamer with 136 channels and an active length of 212.5 m. We began surveying seismic lines crossing the OBS stations and additional profiles for reconstructing the regional salt tectonic-dominated structural setting. We continued shooting 2D seismic profiles on the **21st July** until the morning of th**e 22nd of July**, when we began recovering the OBS. All 15 OBS were on board at noon and we continued with taking eight box core grab samples within and around the crater. Afterwards, we deployed the airgun and a streamer with 136 channels and an active length of 212.5 m again and headed towards a pockmark field approximately 20 nm northeast of the Figge Maar. The 2D seismic surveys were finalized in the morning of the **23rd of July** and we surveyed the area with the multibeam system until the evening. After finishing the multibeam survey, we headed towards Brunsbüttel to enter the Kiel Canal, which we reached in the morning of the **24th of July**. We arrived in Kiel in the afternoon. The **25th of July** was used to calibrate the EK60 fishery echosounder in the Kiel Bay, which was finalized in the afternoon. In the morning of the **26th of July**, the equipment was unloaded on the pier of the east shore campus of GEOMAR.

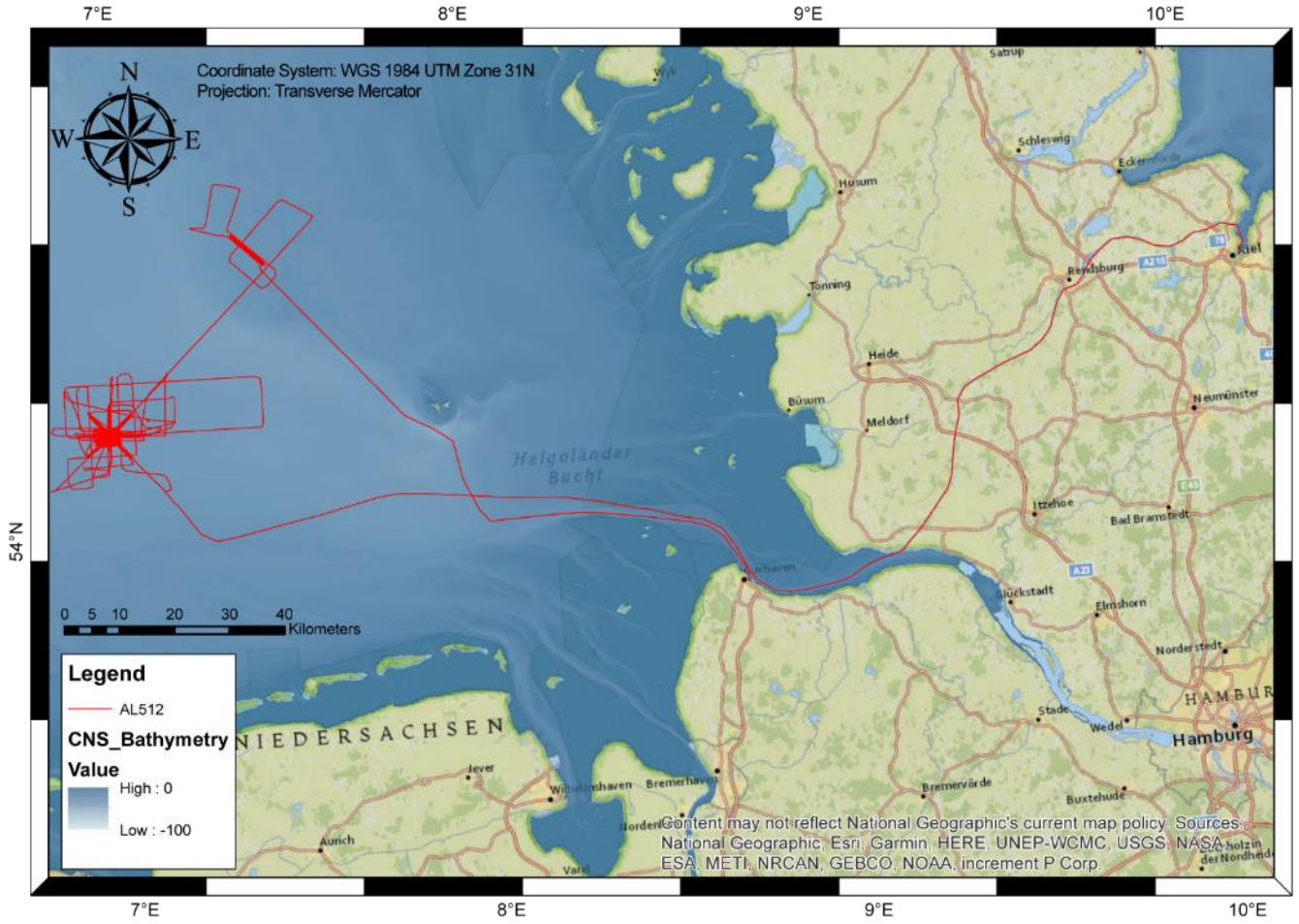

Figure. 3: Cruise track of AL512

3 Participants

Table 1: List of scientific crew

Name	Task	Institute
Dr. Jens Karstens	Chief Scientist, reflection seismics	GEOMAR
Dr. Jens Schneider v.D.	Senior scientist, hydroacoustics	University of Kiel
Christoph Böttner	PhD student, hydroacoustics	GEOMAR
Dr. Judith Elger	Senior scientist, reflection seismics	GEOMAR
Michel Kühn	Master student, reflection seismics	GEOMAR / University of Kiel
Bettina Schramm	PhD student, OBS seismics	GEOMAR
Dr. Benedict Reinardy	Quaternary sedimentology	University of Stockholm
Rebecca Kühn	PhD student	GEOMAR
Helene-Sophie Hilbert	Master student	GEOMAR / University of Kiel
Philipp Müller	Master student	GEOMAR / University of Kiel
Florian Beeck	Technician	GEOMAR
Gero Wetzel	Technician	GEOMAR

Figure 4: Group picture of the scientific crew of AL512

4 Methodology and Preliminary Results

4.1 2D reflection seismic

4.1.1 Methodology

The 2D seismic survey aimed to survey the Figge Maar and to characterize the natural fluid migration pathways and the drilling-induced blowout. During the expedition, a MINI GI-Gun 30 (15 cubic inch generator and 15 cubic inch injector) was used as seismic source. Seismic data were recorded with GeoEel digital streamer segments. Fig. 5 shows the seismic 2D lines acquired during cruise AL512.

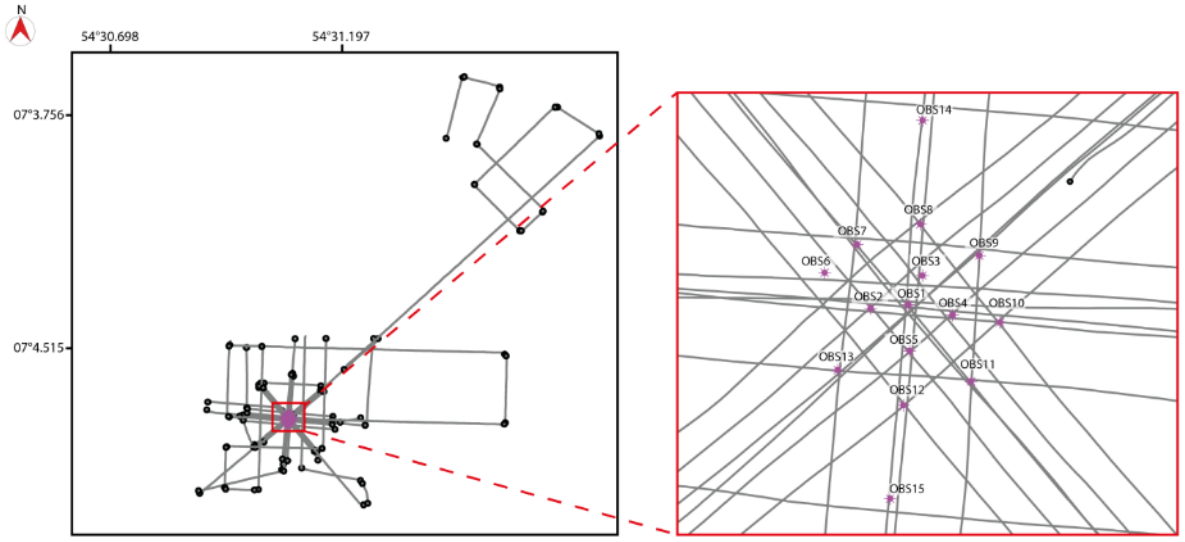

Figure 5: 2D seismic survey lines acquired during the cruise AL512.

Seismic source

During the seismic experiment, we used a "MINI GI-gun 30" with volume reducers in harmonic mode as seismic source. A buoy stabilized the gun in a horizontal position at a water depth of ~2 m (Fig. 6). The gun comprised of 15 in^3 generator and 15 in^3 injector chambers. The release of the injector pulse was triggered with a delay of 25 ms during the 2D seismic data acquisition with respect to the generator pulse. This delay value was adopted for an approximate source depth of 2 m and a gun pressure of 120 bar (1740 psi). We estimated a delay of -40 ms (-27 ms for survey P1000) from the acquired seismic data. The shooting interval was adjusted to 5 seconds, resulting in a shot point distance of 10.3 m with a ship's speed of approximately 4 knots through the water.

Figure 6: Mini GI-Gun (15/15 in3) was operated in harmonic mode as seismic source during AL512.

Streamer system

We used different configurations in digital streamer length (Geometrics GeoEel streamer segments) for recording the seismic signal. Deck geometries, streamer configuration and seismic gun setting for the 2D surveys are illustrated in Fig. 7 to Fig. 9. The surveys P1000 and P6000 both have a streamer length of 212.5 m; survey P4000 has a streamer length of 50 m. The seismic streamer system consists of a tow cable, a 25 m long vibro-stretch section behind the tow cable and 4 to 17 active sections (each 12.5 m long) attached behind the stretch zone. The tow cable had a length of 10 to 20 m behind the vessel's stern (see Fig. 7-9). Each active section contained 8 hydrophones with a group spacing of 1.5625 m. Each active streamer section had an analog-to-digital (AD) converter module. The AD digitizer is a small Linux computer. Communication between the AD digitizer modules and the recording system in the lab was transmitted via TCP/IP protocol. A repeater was located between the deck cable and the tow cable (Lead-In). The streamer power supply unit managed the power supply and communication between the recording system and the AD digitizer modules. For survey P1000 and P6000 birds controlled and monitored the desired streamer depth of 2.5 m. A small buoy was attached to the tail swivel of the 2D streamer for all surveys.

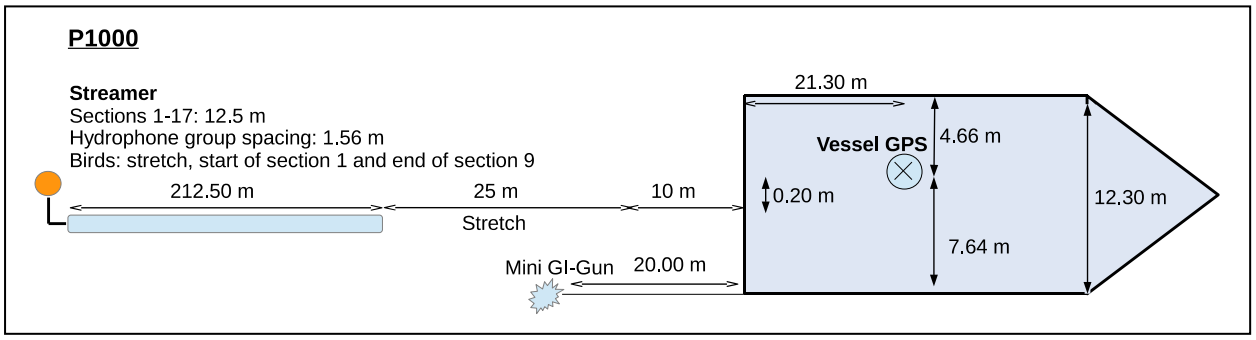

Figure 7: Deck geometries, streamer configuration and gun setting during survey P1000.

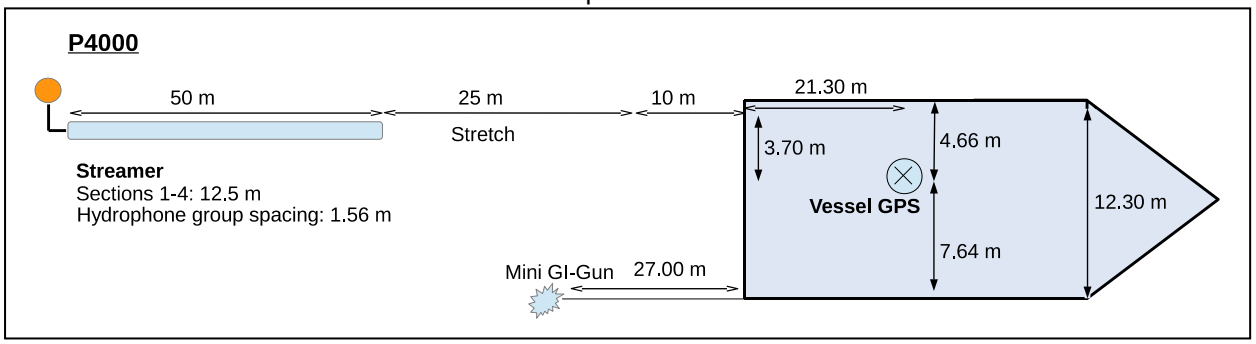

Figure 8: Deck geometries, streamer configuration and gun setting during survey P4000.

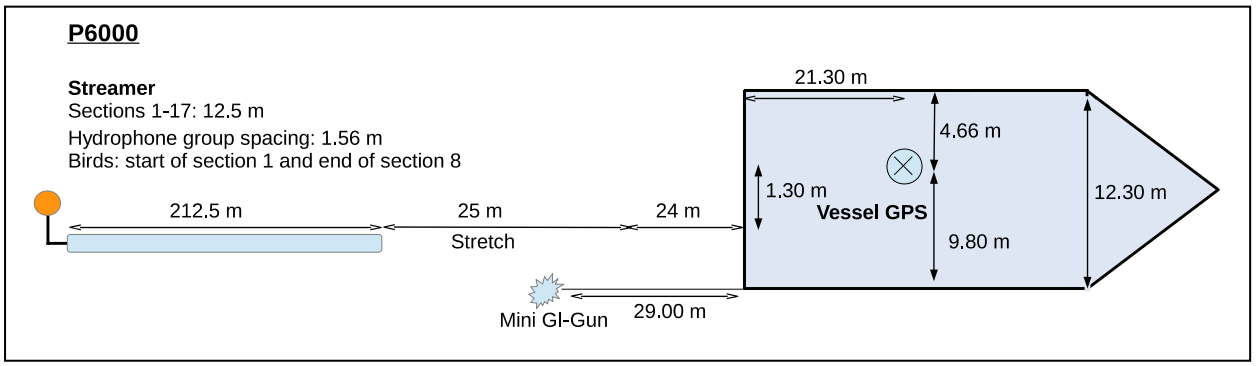

Figure 9: Deck geometries, streamer configuration and gun setting during survey P6000 and P7000.

Bird Controller

Oyo Geospace Bird Remote Units (RUs) were attached to the streamer during survey P1000 and P6000. The schematic locations of the birds are shown in Fig. 7 and 9. The RUs have adjustable wings. A bird controller in the seismic lab controlled the RUs. Controller and RUs communicate via communication coils nested within the streamer. A twisted pair wire within the deck cable connects controller and coils. Designated streamer depth was 2.5 m in accordance with good weather conditions and low swell noise. The RUs thus forced the streamer to the chosen depth by adjusting the wing angles accordingly. The birds worked fairly during survey P1000 but during survey P6000 they kept the streamer at the designated depth.

Data acquisition system

Data were recorded with acquisition software provided by Geometrics. The analogue signal was digitized with 2 kHz. The seismic data were recorded as multiplexed SEG-D. Recording length was 3 seconds during survey P1000 and 4 seconds during surveys P4000, P6000 and P7000. One file with all channels within the streamer configuration was generated per shot. The corresponding logged shot file reports shot number and time information contained in the RMC string. The acquisition PC allowed online quality control by displaying shot gathers, a noise window, and the frequency spectrum of each shot. The cycle time of the shots were displayed as well. The vessel's GPS was simultaneously logged in the RMC string along with logged time and position information.

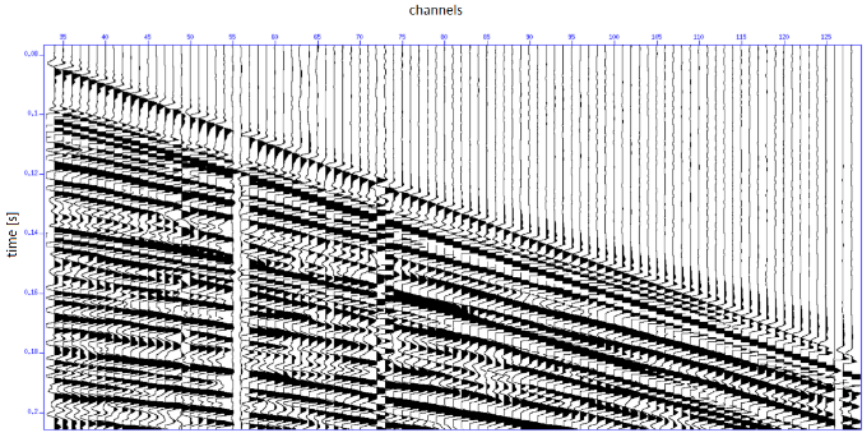

Figure 10: Plot of the seafloor signal for one shot and the first 128 channels and inverse polarity of channel 72.

Processing

On-board processing included streamer geometry configuration, delay calculations and source and receiver depth control. From the seismic data, a delay of -27 ms was calculated for survey P1000 and -40 ms for the other surveys. A receiver ghost effect in the seismic data could not be detected (Fig. 10). The source-receiver locations were then binned with a common-midpoint bin spacing of 1.5625 m. Different filter tests were performed and the frequency spectra (Fig. 11) were analyzed. Seismic traces were balanced and filtered using a bandpass filter with corner frequencies at 20, 70, 300, 550 Hz. Subsequently, a normal move out correction and stacking were applied. From the CTD measurements we derived a mean velocity of 1508 m/s for the water column. The stack was migrated with a 2D Stolt algorithm (1500 m/s constant velocity model). For survey P4000, P6000 and P7000 the assumed geometry of the streamer and the repositioning of the receivers was not precisely enough and thus the normal move out correction could not correct for the offsets and lead to poor stacking results. Using a constant velocity of 1680 m/s improved the stacking result and allowed a first interpretation. For further interpretation, we will need to correct the source receiver offsets.

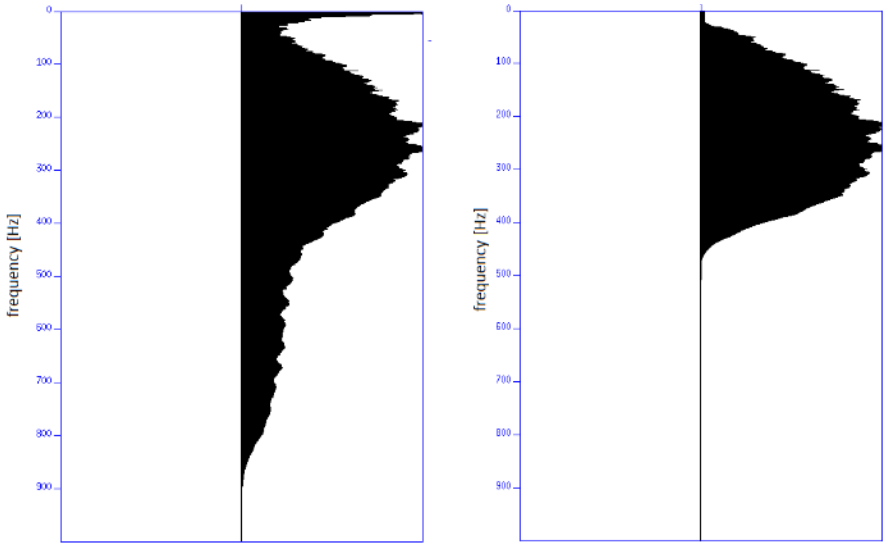

Figure 11: Unfiltered and filtered frequency spectra.

4.1.2 Preliminary Results

Preliminary 2D seismic data show the B1 blowout crater and the underlying stratigraphy. The seafloor reflection in the crater shows a reversed seismic polarity, which indicates high gas content in the pore space. Indications for a front of free gas can be found right next to the crater. At about 0.075 s TWT a reflection, presumably the last glacial unconformity can be observed. Below this unconformity the seismic reflections are steeply dipping. As the seafloor is located at 0.05 s TWT, the first and second multiple of the seafloor are located at 0.1 s TWT and 0.15 s TWT.

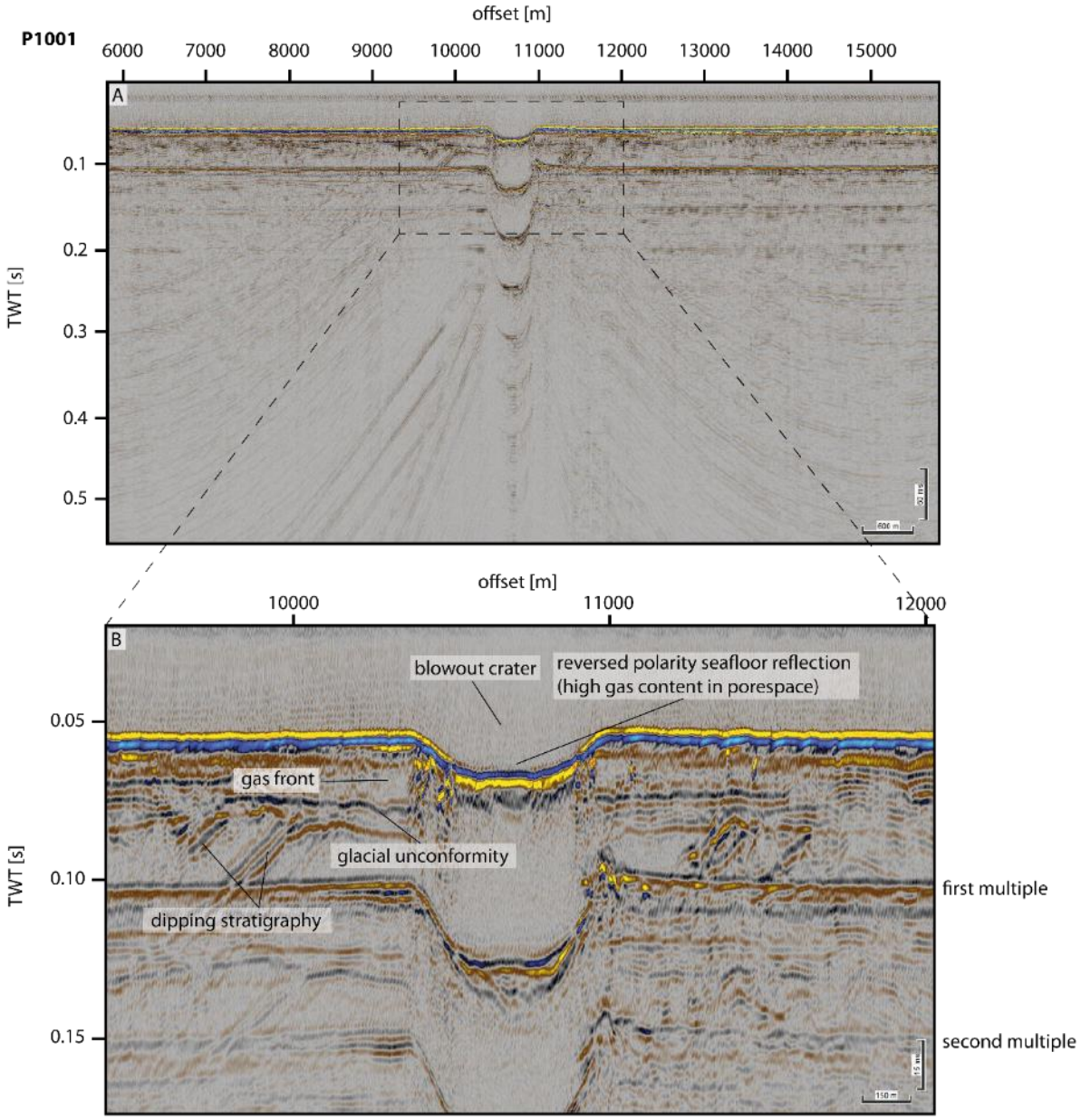

Figure 12: Seismic profile crossing the Figge Maar after initial onboard processing.

4.2 P-Cable 3D seismic

Due to technical problems, no 3D seismic data was acquired with the P-Cable system during AL512.

4.3 Ocean-Bottom-Seismometer

4.3.1 Methodology

The Ocean-Bottom-Seismometer (OBS) consists of four floats, which are connected to a frame and is generally equipped with a three-component seismometer, a hydrophone and a data recorder encased in a high-pressure tube (Fig. 13). All sensors are connected to the recording unit and continuously record the incoming signals. The system itself floats at the sea surface. In order to deploy the device on the ocean bottom a weight is mounted to the frame and attached to a so-called releaser. This releaser has an acoustic communication unit, which can be addressed from the ship in order to disconnect the weight after the experiment. The OBS will then ascend to the surface and can be recovered. A flashlight, radio transmitter and a flag are attached to the frame to increase the visibility of the OBS and to facilitate an easy and quick recovery. While the OBS continuously records seismic signals an additional data logger on board records the corresponding shot times and is used to correlate the results at a later stage of data processing. The data recorders need to be programmed before the deployment of the system. The sample rate of the OBS recorders was set to 500 Hz, while the time logger had a sample rate of 1000 Hz.

The gain of the input channels was set to 16 for the three geophone components and to 1 for the hydrophones. Each recorder was equipped two memory cards between 32 GB and 128 GB. The exact recording parameters for the deployments are listed in Tab. 5 in section 7. The recording units were synchronized with the GPS signal both before and after the recording period to correct for any time shifts within the logger’s internal clock.

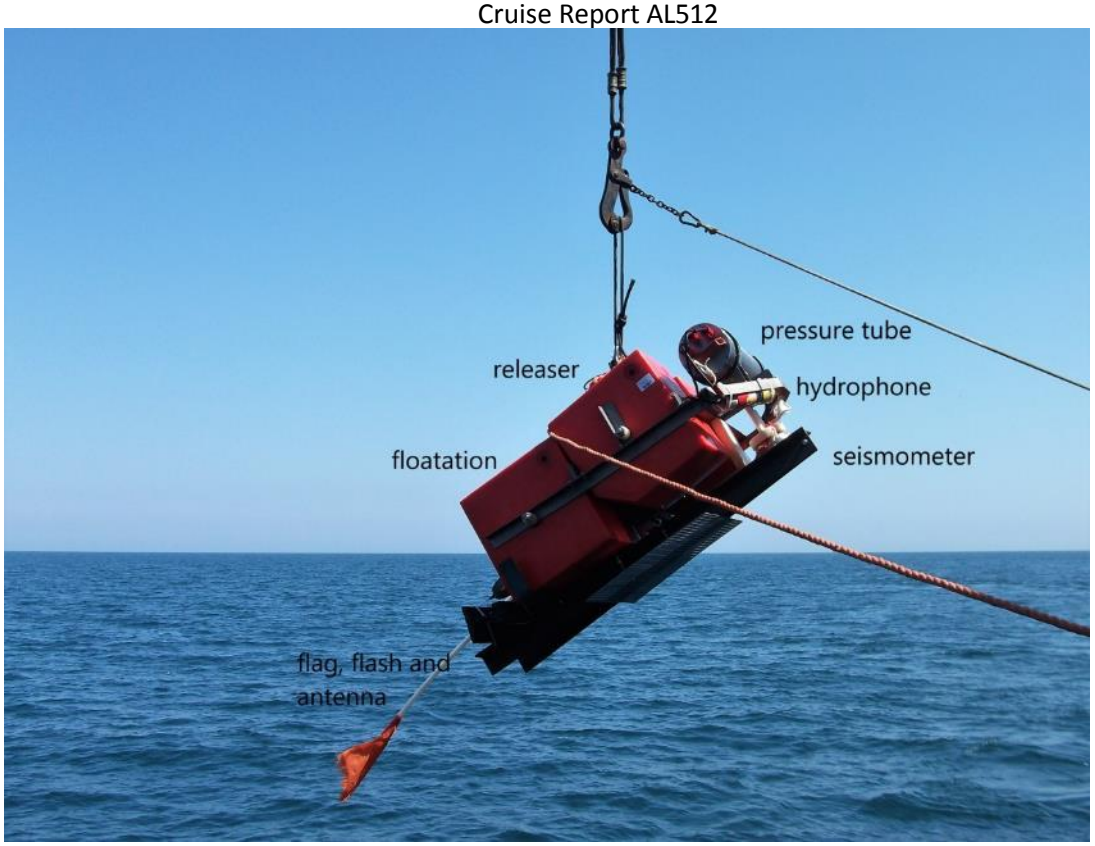

Figure 13: Ocean-Bottom-Seismometer during deployment

4.3.2 Preliminary Results

The main target of the OBS experiment was to provide velocity information for 3D tomography as well as to support further 2D and 3D seismic analyses of the investigation area. We deployed 15 OBS around the Figge Maar on July the 15th 2018 (Fig. 5) in a water depth between 35 and 44 m. We recorded one dedicated linear profile crossing the OBSs (P3001) and three ring profiles (radius 150m, 350m and 750m around the centre of the Figge Maar; centre OBS01) using the Mini-GI-gun with a shot interval of 5 s (Tab 5). Afterwards, we additionally deployed a streamer with four sections to record profiles P4001-P4014 and a streamer with 17 segments to record the profiles P6001-P6024. All 15 OBS were recovered successfully on July the 22nd and the recorders were synchronized. The on board synchronisation of OBS 09 failed, but will be done in Kiel. All data were copied and converted to SEG-Y files on board. First inspection of the data aboard RV ALKOR showed a good data quality, but detailed processing will be carried out after the cruise at GEOMAR. Unfortunately, OBS02 did not record useful data.

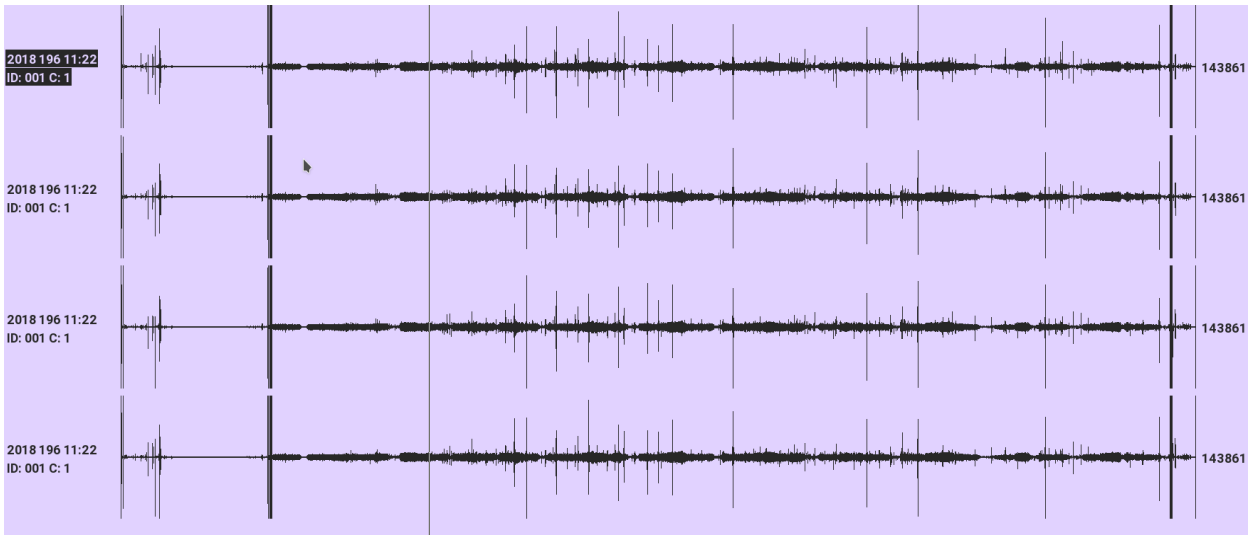

Figure 14: Air gun shots recorded by OBS01. All four channels show a clear signal of the shots.

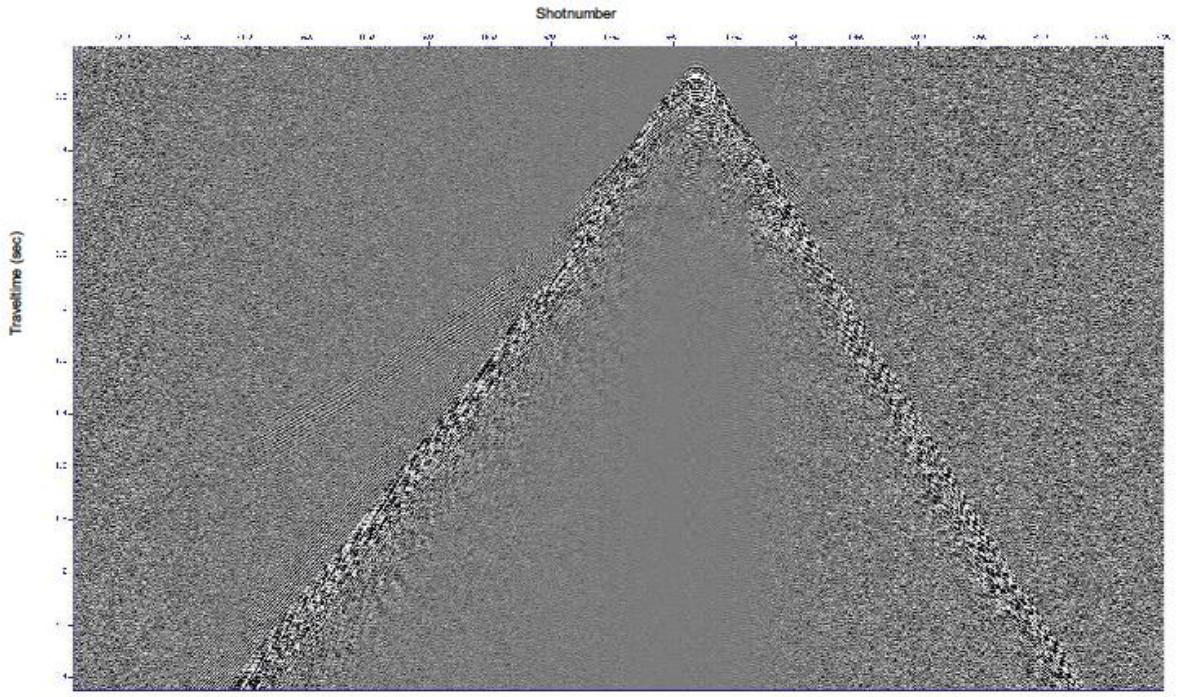

Figure 15: Record section of OBS03. Clear refractions are observed in both offset directions.

4.4 NORBIT Multibeam

4.4.1 Methodology

We installed a NORBIT iWBMSe Wideband Multibeam System (MBES) in the moonpool of R/V ALKOR. The iWBMSe integrates an Applanix Surfmaster motion and inertial navigation system (IMU), as well as a sound velocity probe next to the sonar head. A dual GPS antenna was installed on the top deck of ALKOR and connected to the IMU. Installation offsets on ALKOR were taken from a previous installation (Table 2). Via ALKOR's internet connection, we supplied RTK corrections (18-AXIO-NET) to support the dual antenna GPS recordings.

The NORBIT MBES produces a chirp signal with a 500 µs lasting pulse resulting in 80 kHz bandwidth. 512 beams are formed with beam resolution of 0.9° across-track and 1.9° resolution along-track at 400 kHz. Range resolution can achieve accuracies up to a centimeter in shallow water. We sailed our surveys with 140°-150°. Attitude data (.000 format) were collected with 200 Hz to allow for later post-processing of the IMU data. Hypack 2018 and the NORBIT GUI recorded .hsx and .s7k data in parallel for bathymetry, backscatter, and snippet backscatter. MBSystem and QPS Qimera were applied for post-processing. For assessing vertical profiles of sound velocity we used a multisensor CTD 75M manufactured by Sea & Sun Technology. It is a self-sustaining probe, which is powered by batteries and can operate down to a depth of 1000 m. Three of the eight channels were equipped with a pressure, conductivity, and temperature sensor. Furthermore, the time mode was used to record UTC stamps with a sampling rate of 0.1 s. From the data, we derived the salinity, sound velocity, density, and acoustic absorption values.

Table 2: Installation lever arm offsets between the POSMV Surfmaster within the sonar head and the primary (port) antenna (fixed on the metal bar welded on rail on the top deck of ALKOR).

Applanix coordinates	**Offset [m] to primary antenna on the top deck**
X	3.70
Y	3.52
Z	-16.23

Table 3: Parameter Setup before and after the calibration.

Parameter	**Initial GAMS value**	**Final GAMS value**
Heading Calibration Threshold	3°	3°
Heading Correction	0°	0°
Baseline Vector X	0	0.01
Baseline Vector Y	2.000	1.998
Baseline Vector Z	0	-0.057

4.4.2 Preliminary Results

Multibeam echosounder and IMU performance

After sailing eights for approximately one hour the IMU completed its self-calibration. The IMU also achieved float and fix RTK GPS leading to accuracies up to 5 cm for position and 8 cm for height most of the survey time. The AXIO-Net connection occasionally broke, preferentially at a heading around 70°. The

roll calibration was conducted next to the Figge Maar crater on a flat bottom resulting in -0.61° offset. Patch test lines were also sailed in the second working area to refine the calibration with pitch and yaw offsets. Bathymetric data were recorded with 512 equally distributed beams. Sonar settings were kept constant to allow for proper backscatter analyses (Lurton & Lamarche, 2015). Generally the data suffered in strong interference with the other seismo-acoustic devices operated in parallel most of the time. Bottom detection was reliable within the 140° sector, deteriorated with noise at 150°. Simultaneous recording of bathymetry, sidescan, and snippet sidescan was feasible whereas including water column recording rendered the system unstable. Therefore, we only recorded one dedicated MBES water column imaging dataset (WC.s7k) across the Figge Maar crater (SW-NE lines) at slow survey speed. Bathymetric data were recorded at survey speed between 4-5 knots and ping rates between 3-5 Hz. The heave could not be compensated properly resulting in a +-5 cm uncertainty. We attribute this to performance issues of the Surfmaster IMU, which is not designed for open ocean swell compensations. Heave might be improved by post-processing (true heave) or RTK heave application.

Oceanographic corrections

The water level in the research area is heavily impacted by the M2 tide with approximately ±1 m amplitude. Therefore the OTPS model TPX-O8-Atlas v1 (Fig. 16) was used to calculate a tidal water level time series for correcting the bathymetry. The compensation of the bathymetry with modeled data gave rise to ambitious results. Alternatively, RTK GPS will be used in post-processing to eliminate tidal effects.

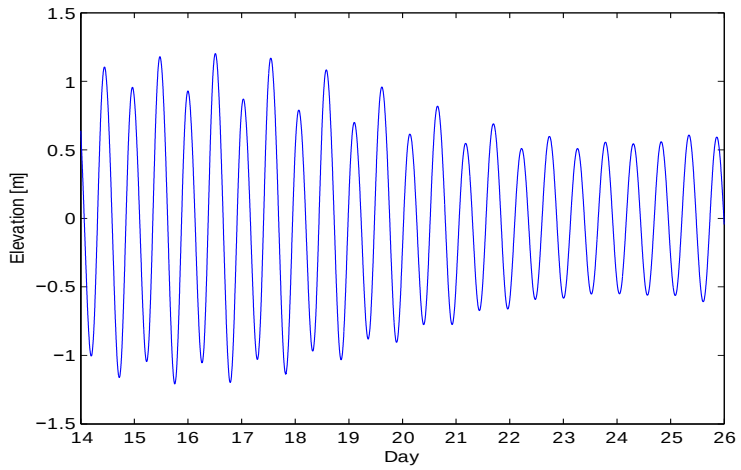

Fig. 16: Modeled water level range predicted for 6° 55' E 54° 8' N between 14th and 26th of July, 2018. Resolution of the applied Ocean Tidal Prediction Model (OTPS, Oregon state University) is 1/30tiest of a degree resolution for the North Sea.

The water column in the German Bight is considered to be mixed throughout the year (Holt and Umlauf, 2008). Nonetheless some stratification is visible in our CTD cast (Fig. 17) resulting in a sound speed range between 1500 m/s at depth and 1521 m/s, likely temperature driven. Eight CTD casts have been conducted in the proximal and distal domain (0-3 nm) around the Figge Maar blowout crater.

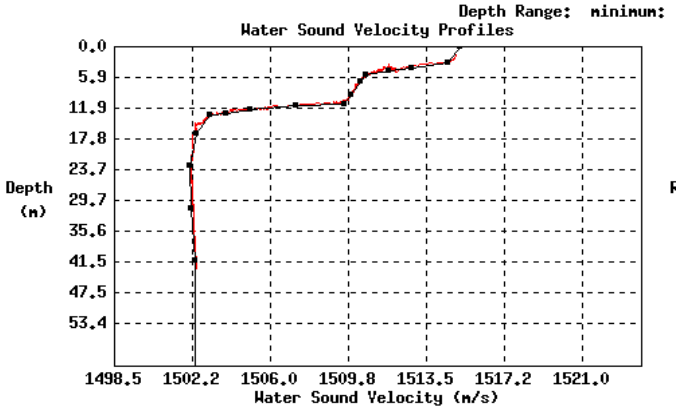

Fig. 17: Sound velocity profile calculated after the UNESCO formula.

Bathymetry and backscatter of the Figge Maar **blowout crater**

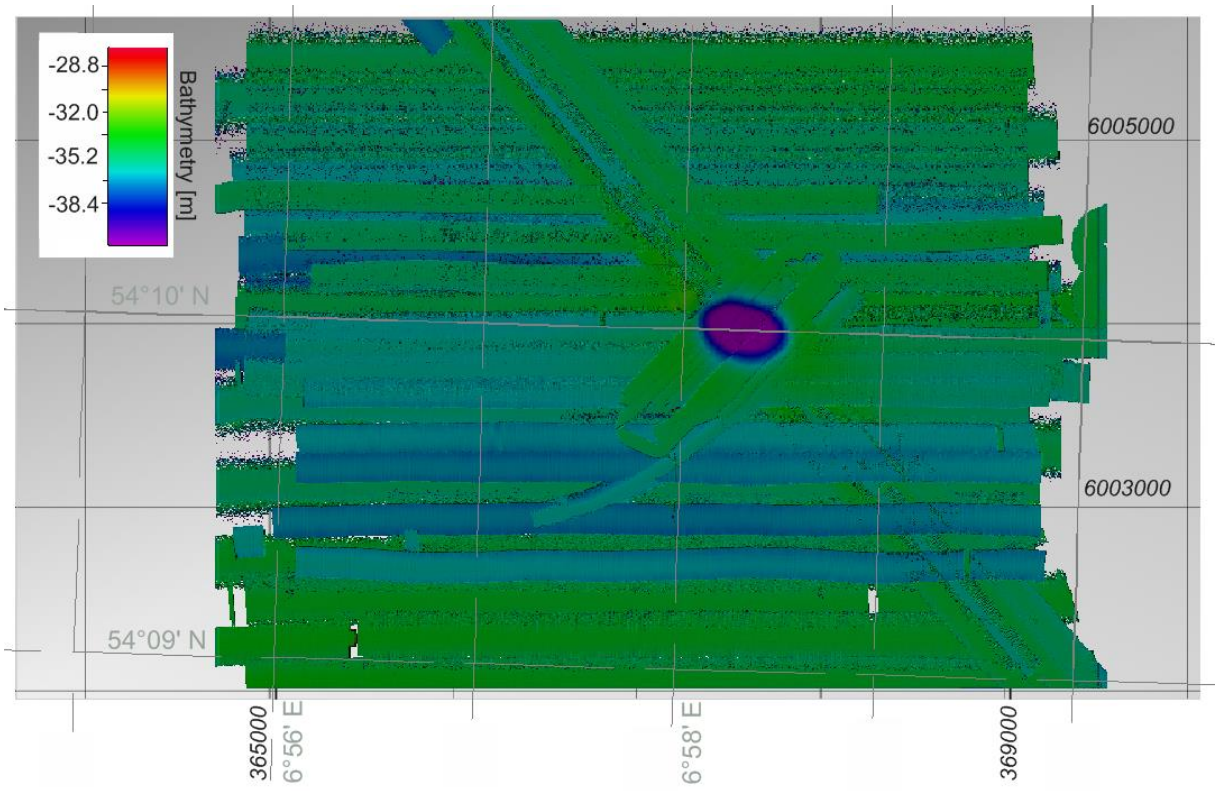

Fig. 18: Bathymetric overview chart showing the Figge Maar *crater with a maximum water depth of -44.5 m within the flat seafloor with mean water depth of 35.5 m. Tidal water level changes have not been compensated for this chart. UTM32N projection has been applied, axis and labels show UTM and geographic coordinates (WGS84), respectively.*

A rectangular area of 2 by 2.5 nm was mapped surrounding the Figge Maar blowout crater site. The sandy seafloor (groundtruthed by sediment sampling) appears flat and featureless with a mean depth around 35.5 m. The crater is characterized by an elliptical shape with minor and major axes length of 460 and 565 m with the major axis striking NW-SE. The maximum depth of the crater was measured with -44.5 m below sea level. Comparing to the deepest sounding of 50.9 m and shape assessed in 1995 (Thatje et al., 1999) we find a 6.4 m depth offset and suggest that this resulted from crater wall erosion and infill from the surroundings. If averaged over the past 23 years the 6.4 m offset would transform into an exceptional

sedimentation rate of 278 mm/yr.

The slope across the crater reaches values between 3 and 7° with the steepest slope on the southeasterly flank. The rim shoulder of the crater appears elevated with a 0.5 – 1 m thick levee revealing horizontal layering in the subbottom data (Fig. 19).

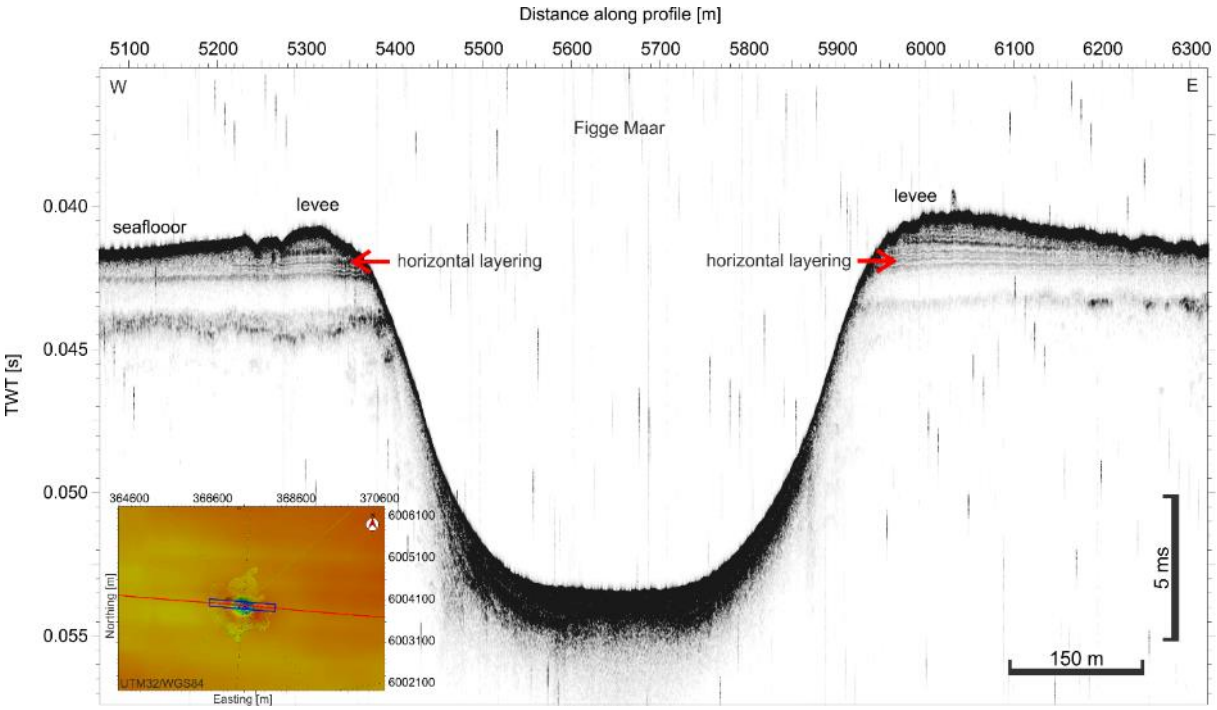

Fig. 19: 1.2 km-long SES profile across the Figge Maar crater from West to East showing the internal layering of the 0.5-1 m thick levees. The inset shows the location of the profile.

The levee can hardly be explained as a sand wave feature, because it shows strong horizontal layering. A little pockmark was identified south of the crater. Acoustic water column analyses will clarify if active gas venting is present.

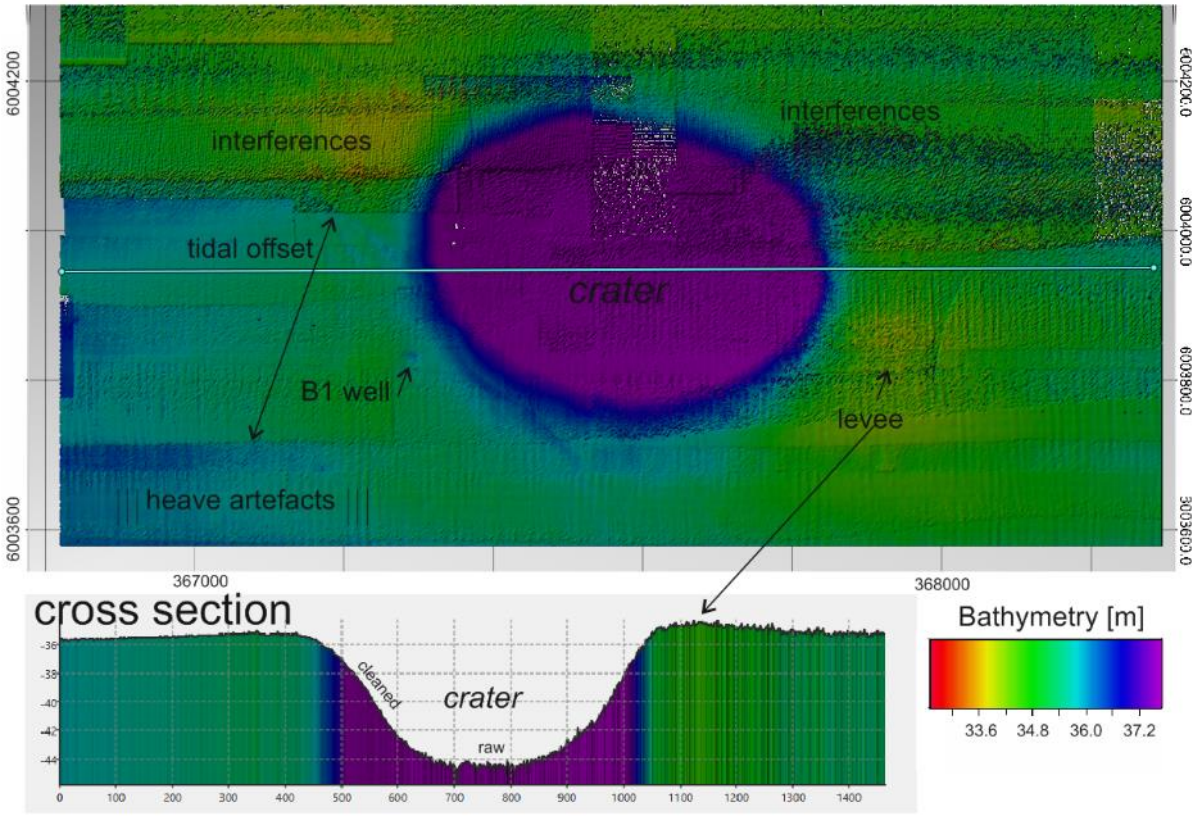

Fig. 20: Close-up bathymetry of the B1 crater and a cross section drawn from west to east (blue line). Tidal effects have been corrected by data shown in Fig. TIDAL. Though, tidal offsets of appr. 30 cm are still visible. Soundings were partly edited (cleaned) in the southwestern part of the figure.

The backscatter of the working area can be separated into three zones. Within the crater the backscatter is generally low with a few elongated positive acoustic anomalies in a meter scale that became visible online in the 400 kHz MBES snippet imagery. Given the abundant findings of benthic fauna within the crater, we suggest that the acoustic anomalies are associated with biogenic activity. The crater rim and the proximal area surrounding the crater within a 150 m radius show high backscatter characterized by texture linearity in northwest-southeast direction, similar like the orientation of the major axis of the ellipsoidal crater. The backscatter amplitude distribution is in line with preliminary analyses of grab samples indicating that the sand fraction on the rim is higher than in the crater. Approximately 100 m southwest away from the crater rim a seafloor anomaly was found likely caused by well site structure from the former drill site B1. In the distal domain of the crater and within the 2 by 2.5 nm survey area a homogeneously distributed intermediate backscatter was found with dozens of trawl marks.

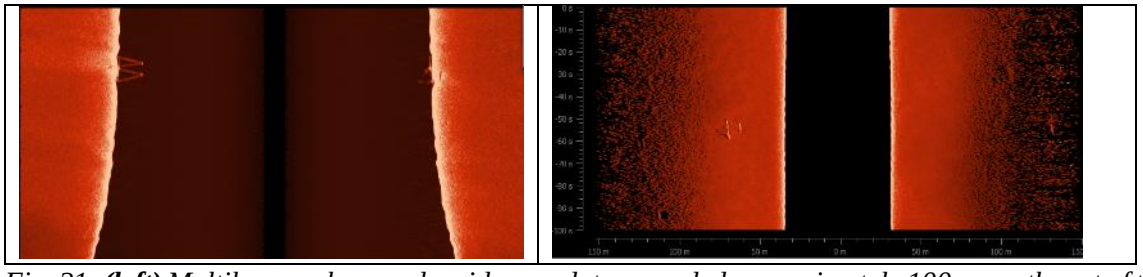

*Fig. 21: **(left)** Multibeam echosounder sidescan data recorded approximately 100 m southwest of the crater crim. The sidescan shows a dedicated anomaly in the water column at the well site. **(right)** Multibeam echosounder snippet-sidescan data showing the anomaly with a precise beam geo-location on the seabed.*

Bathymetry of the pockmark field

Given the failure of the 3D seismic surveying, an alternative research field was chosen 30 km northeast of the blowout crater. The area was reported to be characterized by up to 1.200 pockmarks per square kilometer (Krämer et al., 2017) and we run several multibeam and subbottom lines to further evaluate the dynamics of this area.

4.5 INNOMAR Sediment echosounder

4.5.1 Methodology

The seismic profiles were recorded together with a parametric subbottom profiler of type Innomar SES-2000® medium. This device is hull-mounted on R/V ALKOR. It transmits two high frequencies at high sound pressure. These two sound waves interact in the water column, generating harmonics. The SES-2000® medium sends and records primary frequencies of about 100 kHz and thus generates parametric secondary frequencies within the range of 4 – 15 kHz. Secondary frequencies develop through nonlinear acoustic interaction of the primary waves at high signal amplitudes. The advantage of these secondary frequencies is that they have a similar beam width and short pulse lengths as the primaries despite the low frequency and the small transducer. The system allows a simultaneous acquisition of up to three different frequencies (multi-frequency mode), which are shot sequentially. Every shot records two channels comprising a primary high frequency (HF) and secondary low frequency (LF) as full waveform and envelope. The secondary frequencies are adjustable and were set to 4 kHz with two pulses and 15 kHz with one pulse during all surveys. The system has a vertical resolution of 6 cm and its accuracy depends on the frequency and water depth, e.g. 100/10 kHz: 2/4 cm + 0.02% of the water depth (Wunderlich and Müller, 2003). The soundings are corrected for heave, roll and pitch movements of the vessel. The system worked reliable and produced high-quality data throughout the whole time.

After recording, the full waveform data were converted into the segy-format with SES-convert (version 2.3.0.2). If seismic data were collected simultaneously, one SEG-Y file was created for the length of each seismic profile. We imported the converted segy-files into IHS Kingdom seismic interpretation software and calculated the envelope subsequently.

4.5.2 Preliminary Results

At the survey area, the INNOMAR SES- 2000® medium was mainly used for analysis of sedimentary processes of the upper most sedimentary succession. These processes include the identification of different phases of glacial deposition or erosion and sedimentation history of the Figge Maar blowout site. Despite the expected coarse-grained material and glacial tills on the North Sea seafloor, the system showed very good penetration depth with very high resolution.

The sedimentary succession in the survey area is very heterogeneous, but shows at least three major seismo-stratigraphic units. The topmost Holocene sediments are characterized by strong seismic reflections, transparent seismic facies, are present throughout the whole survey area and vary strongly in thickness (Fig. 22). The underlying chaotic to transparent unit with a corrugated surface likely corresponds to glacial sediments of Pleistocene age. The parametric sediment echosounder shows very low penetration rates into this unit due to the coarse grained, poorly sorted sediment and subsequent high acoustic impedance

contrast. Approximately 5 nm northeast of the Figge Maar, the glacial sediments show various areas, where the Holocene and Pleistocene sedimentary units are separated by a well-laminated seismic unit, likely corresponding to glacio-marine sediments. The seismic facies of this glacio-marine sediments show top lap of seismic reflection towards the Holocene sediments, indicating an erosional surface.

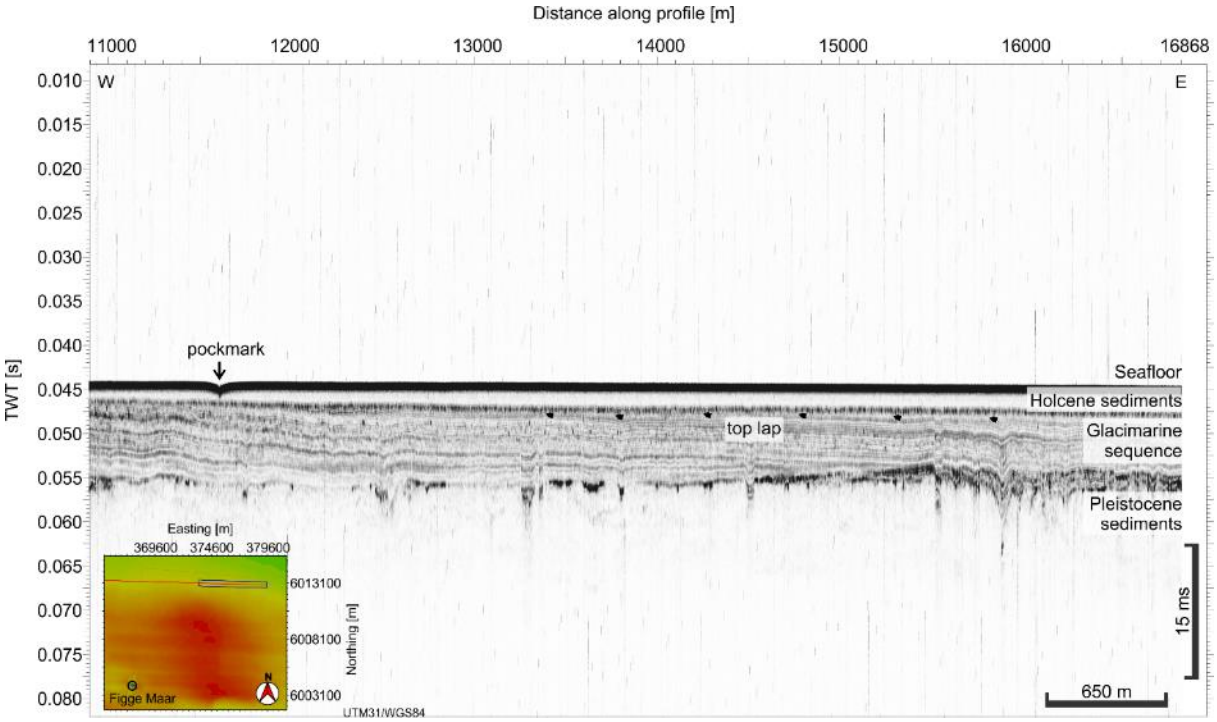

Fig. 22: INNOMAR SES-2000 medium profile with 4 kHz (LF1) showing the shallow background stratigraphy of the study area. Map on left lower corner shows location of profile in UTM [m] Easting/Northing (UTM zone 31, WGS 84).

Our parametric echosounder shows well-laminated stratigraphic layer within the blowout crater. The flanks of the initial blowout are visible at the rim of the recent crater, enabling a reconstruction of sedimentation since blowout initiation. These flanks show little sedimentation in comparison to the crater center. The recent crater is surrounded by a 1-4 m elevated circular levee, which shows well-laminated seismic reflections. This levee is more pronounced in eastern and western direction off the Figge Maar. On the western side, the levee shows a corrugated surface, possibly indicating sediment waves. A seismic chaotic to transparent unit, likely representing the initial blowout sediments of the Figge Maar, underlies the levee.

The parametric sediment echosounder is highly sensitive to gas in pore space and thus can be used to map shallow gas accumulations. There are various sites where gas flares in the water column coincide with bright spots in the shallow (< 5 m) sedimentary succession. South of the Figge Maar the acoustic turbidity is highest and shows clear correlation with flares in the water column. The sediments inside the crater show well-laminated seismic reflections which are disturbed at approximately 2 ms beneath the seafloor (corresponding to 1.5 m at 1500 m/s) by acoustic turbidity. Inside the crater, the acoustic turbidity is shallowest beneath the center and deepest on the outer parts. At the center of the Figge Maar and 10 ms TWT (corresponding to 7.5 m at 1500 m/s) beneath the seafloor our data shows patches of high-amplitude reflections with polarity reversals (bright spots), indicating a shallow situated reservoir of free gas. Whether this is the original source of the released methane or if this is an intermediate reservoir is beyond the penetration depth of the parametric echosounder.

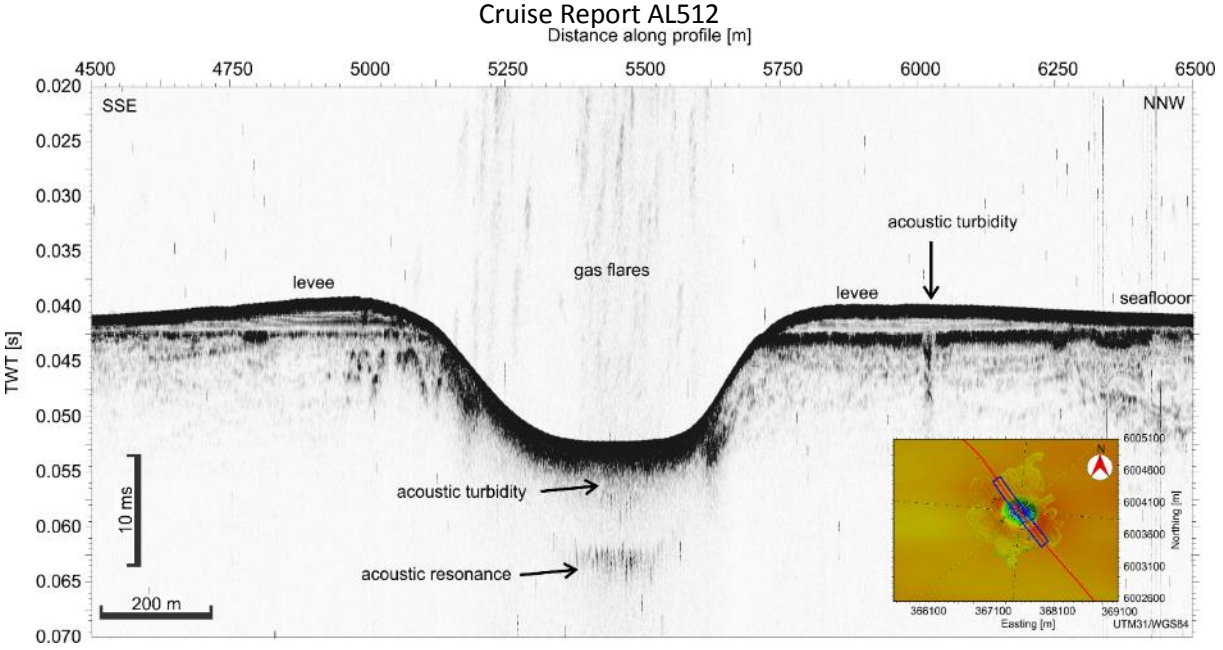

Fig. 23: 2 km-long INNOMAR SES-2000 medium profile with 4 kHz (LF1) crossing the Figge Maar from south-southeast to north-northwest. Map on right lower corner shows location of profile in UTM [m] Easting/Northing (UTM zone 31, WGS 84).

The very high-resolution imaging of the INNOMAR SES- 2000® medium enabled an identification of different seafloor-based structures, such as the wellhead of well B1 or OBSs.

4.6 EK 60 fishery echosounder

4.6.1 Methodology

The fixed installed fishery echosounder KONGSBERG EK60 was operated with all frequencies (38, 70, 120, and 200 kHz) for gas bubble flare imaging. Pulse length and power were set constant throughout the cruise (Tab. 4). The survey speed was occasionally reduced to less than 1 knot to enhance bubble detection and to allow for individual bubble trajectory imaging, analyses and thus gas seepage characterization.

4.6.2 Preliminary Results

Calibration

The four split-beam sonar transducers on R/V ALKOR were calibrated with copper spheres of known target strength (TS) after the cruise on 25th July 2018 in Kiel to obtain absolute target strength (TS). The temperature and salinity were estimated 18° and 14 ppt respectively at the spheres position between 12-15m water depth. This results in a sound speed of ~ 1495 m/s. Next to this value, the TS versus sound speed diagram shows a plateau, which makes the estimate robust in terms of a missing CTD cast. For logistical reasons, a CTD was only taken after the calibration that can be used to rerun the calibration with the recorded raw files. Though, the resulting RMS values demonstrate a very reliable calibration result (low RMS values; Tab. 4; Fig 24).

Table 4: Sonar settings and calibration results. Values better than 0.2 indicate a very good calibration accuracy, which applies for three of the four frequencies. The results will be used to post-calibrate echo backscattering strength recorded during AL512 to obtain absolute gas bubble target strength values.

Frequency [kHz]	Pulse length [µs]/Power[W]	RMS deviation from beam model [dB]	Ref. Target [dB]
38	512/2000	0.14	-33.6
70	256/1000	0.12	-39.2
120	256/500	0.13	-40.5
200	128/300	0.28	-45.1

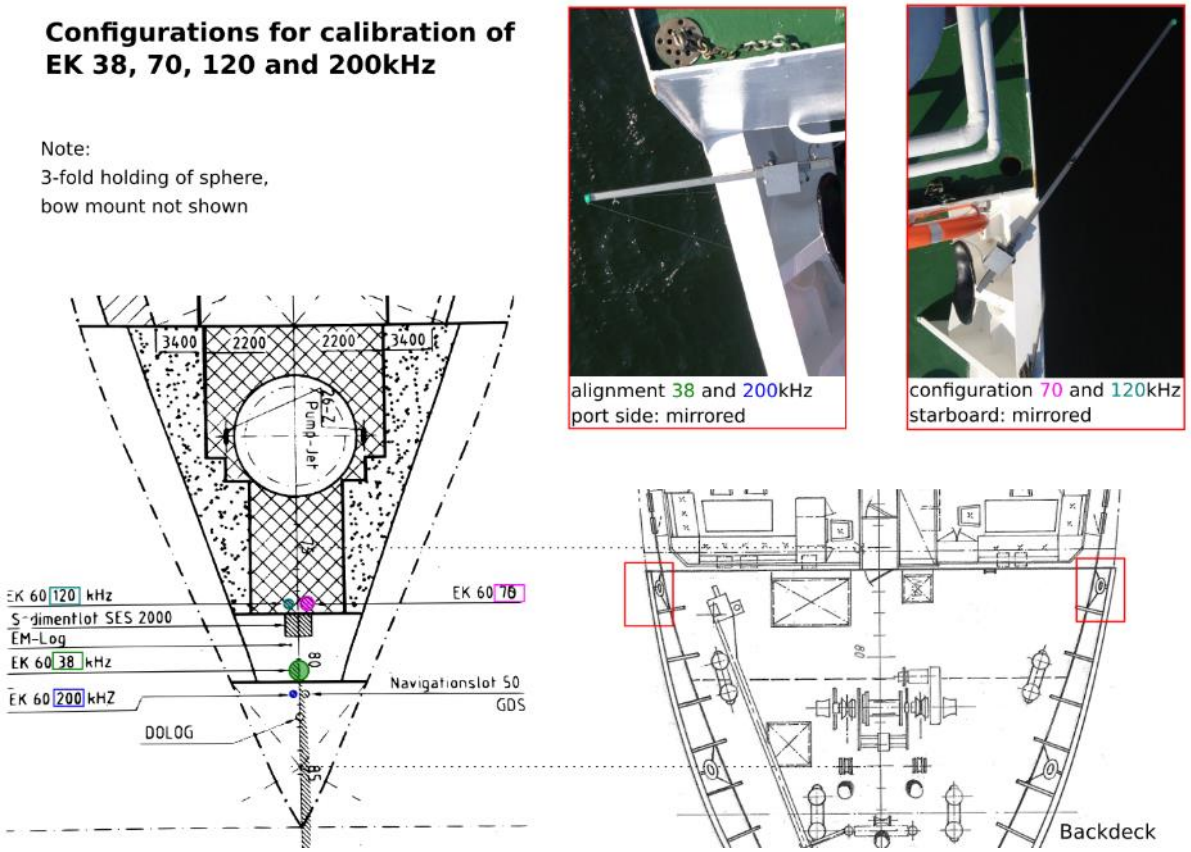

Fig. 24: Setup of the transducer positions on R/V ALKOR (bow of vessel) together. Pictures mark the ideal positions for the rig to steer the sphere into the dedicated transducer (frequency) beam.

Flare imaging

Gas bubble releases from the B1 crater have been reported before (Linke & Haeckel, 2018) and were verified during this cruise. Gas releases were sampled during the previous cruise and were found to consist of methane contrasting the nitrogen gas release that blew the crater out 54 years ago (Linke & Haeckel, 2018). We sailed the profiles with a snail's pace survey speed (<2 knots) to produce characteristic acoustic gas bubble trajectories (Fig. 25). Thus, vertically aligned acoustic single targets emerged in the water column (Fig. 25). Such unambiguous acoustic targets can later be inverted into vertical gas flux with calibrated backscatter soundings. Bubble rise velocities were derived from the trajectories to 20-30 cm/s thus resembling typical values for minor gas bubble releases.

Various gas seep locations and rise heights were mapped and some gas bubbles reached the surface, visible at the sea surface during calm sea. Most gas seeps were counted within the crater. To account for potential temporal and possible tidal effects the crater was surveyed over a tidal cycle and such data will be evaluated in the near future.

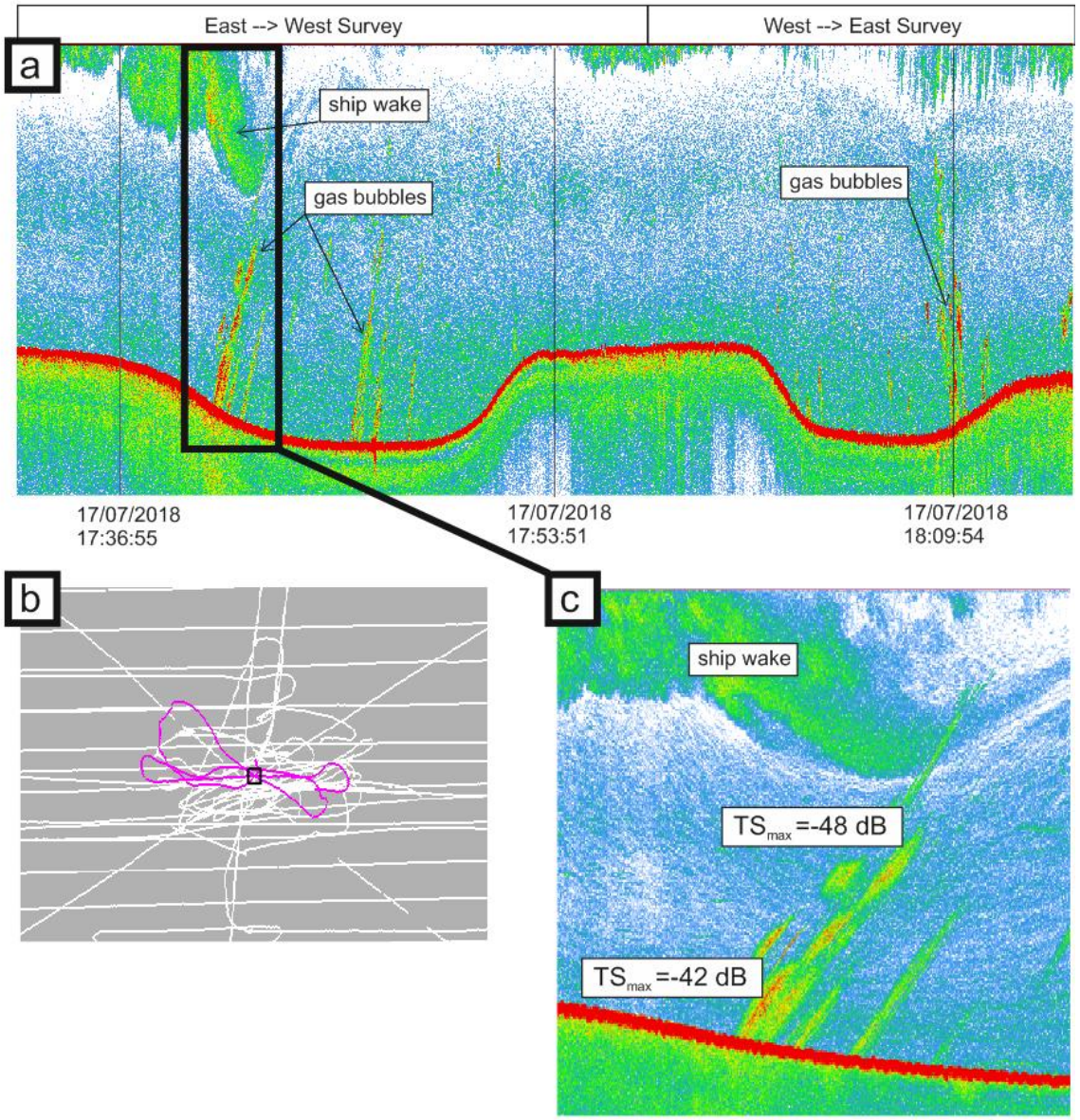

Fig. 25: ***(a)*** *Echogram of the 200 kHz EK60 survey recorded during a snail's pace survey crossing the crater with very slow speed. Gas bubble releases plot with various orientation on the echogram given the varying bubble-survey-current geometry and vessel speed* ***(b)*** *Criss-cross ship survey lines around the crater* ***(c)*** *close up of* ***(a)***.

4.7 Box core sediment sampling

Seven box cores were collected in and around the Figge Maar pockmark. The central part of the pockmark contained primarily mud while the sides of the pockmark contained sandy muds. A levee surrounding the pockmark contained sandy mud to sand. Both sea urchin and mussel shells were relatively abundant, sometimes with high concentrations of shell fragments. Some plant remains were also recovered including fragments of preserved wood. One additional box core was collected outside the pockmark as a reference for the surrounding sea bed and contained sandy mud. The samples will analyzed sedimentologically at University of Stockholm.

5 References

Arntsen, B., Wensaas, L., Løseth, H., & Hermanrud, C., 2007. Seismic modeling of gas chimneys. Geophysics, 72(5), SM251-SM259.

Berndt, C., 2005. Focused fluid flow in passive continental margins. Philosophical Transactions of the Royal Society a: Mathematical, Physical and Engineering Sciences, 363(1837), 2855–2871.

Cartwright, J.A., Huuse, M., Aplin, A., 2007. Seal bypass systems. Bulletin 91, 1141–1166.

Clayton, C.J., Hay, S.J., 1994. Migration mechanisms from accumulation to surface. Bulletin of the Geological Society of Denmark 41, 12–23.

Granli, J.R., Arntsen, B., Sollid, A., Hilde, E., 1999. Imaging through gas-filled sediments using marine shear-wave data. Geophysics 64, 668–677.

Holt, J., & Umlauf, L. 2008. Modelling the tidal mixing fronts and seasonal stratification of the Northwest European Continental shelf. Continental Shelf Research, 28(7), 887-903.

Judd, A., Hovland, M., 2007. Seabed fluid flow: the impact on geology, biology and the marine environment. Cambridge University Press, Cambridge.

Karstens, J., Berndt, C., 2015. Seismic chimneys in the Southern Viking Graben – Implications for palaeo fluid migration and overpressure evolution. Earth and Planetary Science Letters 412, 88–100.

Karstens, J., Ahmed, W., Berndt, C., and Class, H., 2017. Focused fluid flow and the sub-seabed storage of CO2: Evaluating the leakage potential of seismic chimney structures for the Sleipner CO2 storage operation. Marine and Petroleum Geology, v. 88, pp. 81 - 93. doi.org/10.1016/j.marpetgeo.2017.08.003.

Kornfeld, J.A., 1964. Wild blowout taps first North Sea gas. World Oil. August 1, 1964.

Krämer, K., Holler, P., Herbst, G., Bratek, A., Ahmerkamp, S., Neumann, A., ... & Winter, C., 2017. Abrupt emergence of a large pockmark field in the German Bight, southeastern North Sea. Scientific reports, 7(1), 5150.

Leifer and Judd, 2015. The UK22/4b blowout 20 years on: Investigations of continuing methane emissions from sub-seabed to the atmosphere in a North Sea context. Marine And Petroleum Geology 68, 706-717.

Linke, Peter und Haeckel, Matthias, eds., 2018. RV POSEIDON Fahrtbericht / Cruise Report POS518: Baseline Study for the Environmental Monitoring of Subseafloor CO2 Storage Operations, Leg 1: Bremerhaven – Bremerhaven (Germany) 25.09.-11.10.2017, Leg 2: Bremerhaven – Kiel (Germany) 12.10.-28.10.2017. . GEOMAR Report, N. Ser. 040 . GEOMAR Helmholtz-Zentrum für Ozeanforschung, Kiel, 84 pp. DOI 10.3289/GEOMAR_REP_NS_40_2018.

Løseth H., Gading, M., Wensaas, L., 2009. Hydrocarbon leakage interpreted on seismic data. Marine and Petroleum Geology 26, 1304–1319.

Lurton, X.; Lamarche, G. (Eds), 2015. Backscatter measurements by seafloor mapping sonars. Guidelines and Recommendations. 200p. http://geohab.org/wp-content/uploads/2014/05/BSWG- REPORT-MAY2015.pdf

Plaza-Faverola, A., Bünz, S., Mienert, J., 2011. Repeated fluid expulsion through sub-seabed chimneys offshore Norway in response to glacial cycles. Earth and Planetary Science Letters 305, 297–308.

Schneider von Deimling, J. S., Linke, P., Schmidt, M., & Rehder, G., 2015. Ongoing methane discharge at well site 22/4b (North Sea) and discovery of a spiral vortex bubble plume motion. Marine and Petroleum Geology, 68, 718-730.

Thatje , S., Gerdes, D., Rachor, E., 1999. A seafloor crater in the German Bight and its effects on the benthos. Helgoland Marine Research 53, 36-44.

Wunderlich, J., Müller, S., 2003. High-resolution sub-bottom profiling using parametric acoustics. International Ocean Systems 7, 6–11.

6 Acknowledgements

We would like to thank Captain Friedhelm von Staa and the entire crew of R/V ALKOR for their excellent support and hospitality during the entire cruise. Our experiments required advanced maneuvering within a highly tide and traffic-affected area in the North Sea, which have been fulfilled by the bridge to our fullest satisfaction. We would like to thank crew on deck, in the machine and the caboose for providing an encouraging and supportive working environment. This cruise was funded from GEOMAR, Helmholtz-Centre for Ocean Science Kiel through the EU funded project STEMM-CCS und der grant agreement n°654462.

7 Acquisition protocols

Tab. 5: Ocean-Bottom-Seismometer acquisition protocol

	Deployment latitude	longitude	water-depth	**Recovery** latitude	longitude	water-depth	Recorder
OBS01	54°10.020	06°58.275	44	54°09.965	06°58.440	43	GEOLOG
OBS02	54°10.010	06°58.138	40	54°09.979	06°58.120	40	GEOLOG
OBS03	54°10.083	06°58.323	39	54°10.116	06°58.317	37	GEOLOG
OBS04	54°10.001	06°58.436	44	64°10.053	06°58.361	40	GEOLOG
OBS05	54°09.922	06°58.284	41	54°09.924	06°58.282	42	GEOLOG
OBS06	54°10.083	06°57.968	35	54°10.076	06°57.952	35	GEOLOG
OBS07	54°10.145	06°58.083	36	54°10.161	06°58.078	36	GEOLOG
OBS08	54°10.192	06°58.310	37	54°10.188	06°58.341	36	GEOLOG
OBS09	54°10.192	06°58.527	37	54°10.143	06°58.508	36	GEOLOG
OBS10	54°09.988	06°58.609	36	54°10.002	06°58.580	35	GEOLOG
OBS11	54°09.861	06°58.510	36	54°09.859	06°58.431	36	GEOLOG
OBS12	54°09.806	06°58.267	36	54°09.809	06°58.184	36	GEOLOG
OBS13	54°09.877	06°58.025	36	54°09.871	06°57.936	35	GEOLOG
OBS14	54°10.413	06°58.307	37	54°10.417	06°58.196	36	GEOLOG
OBS15	54°09.607	06°58.229	37	54°09.603	06°58.150	36	GEOLOG

Tab. 6: Seismic acquisition protocol

Line #	Start	End	Lat Start N	Long Start E	Lat End N	Long End E	Comment	Rec Len [s]	shot rate [s]
1001	15.07.2018 18:45	15.07.2018 21:13	54° 10.311	06° 49.281	54° 09.702	07° 07.309	17 streamer	3	5
1002	15.07.2018 21:16	15.07.2018 22:38	54° 09.987	07° 07.592	54° 15.404	07° 08.008	17 streamer	3	5
1003	15.07.2018 22:59	16.07.2018 02:33	54° 15.284	07° 07.990	54° 04.890	06° 48.510	17 streamer	3	5
1004	16.07.2018 02:48	16.07.2018 04:02	54° 04.920	06° 48.630	54° 06.410	06° 57.670	17 streamer	3	5
1005	16.07.2018 04:08	16.07.2018 06:06	54° 06.720	06° 55.810	54° 15.721	06° 58.831	17 streamer	3	5
3000a (circle)	18.07.2018 07:11	18.07.2018 07:18	54° 10.059	06° 58.154	54° 09.922	06° 58.255	no streamer		5
3000b (circle)	18.07.2018 07:23	18.07.2018 07:43	54° 10.097	06° 57.951	54° 10.090	06° 57.950	no streamer		5
3000c (circle)	18.07.2018 07:53	18.07.2018 08:52	54° 10.522	06° 57.919	54° 10.326	06° 57.528	no streamer		5
3001	18.07.2018 09:46	18.07.2018 11:19	54° 13.049	06° 58.621	54° 06.723	06° 57.054	no streamer		5
4001	18.07.2018 14:16	18.07.2018 15:36	54° 07.820	07° 00.800	54° 12.059	06° 54.847	4 streamer	4	5
4002	18.07.2018 15:42	18.07.2018 17:07	54° 12.169	06° 54.930	54° 07.891	07° 01.483	4 streamer	4	5
4003	18.07.2018 17:14	18.07.2018 18:37	54° 07.912	07° 01.756	54° 12.260	06° 55.149	4 streamer	4	5
4004	18.07.2018 18:48	18.07.2018 20:10	54° 12.141	06° 54.910	54° 07.826	07° 01.457	4 streamer	4	5

4005	18.07.2018 20:19	18.07.2018 21:41	54° 07.905	07° 01.957	54° 12.233	06° 55.020	4 streamer	4	5
4006	18.07.2018 21:41	18.07.2018 22:40	54° 12.233	06° 55.020	54° 12.396	07° 01.654	4 streamer	4	5
4007	18.07.2018 22:53	19.07.2018 00:19	54° 11.979	07° 01.785	54° 08.160	06° 54.442	4 streamer	4	5
4008	19.07.2018 00:31	19.07.2018 01:27	54° 08.199	06° 54.817	54° 10.840	06° 59.915	4 streamer	4	5
4009	19.07.2018 02:04	19.07.2018 02:34	54° 10.461	06° 59.161	54° 11.930	07° 01.940	4 streamer	4	5
4010	19.07.2018 02:43	19.07.2018 03:58	54° 11.882	07° 02.236	54° 08.390	06° 55.541	4 streamer	4	5
4011	19.07.2018 04:31	19.07.2018 05:55	54° 08.163	06° 54.465	54° 11.966	06° 01.884	4 streamer	4	5
4012	19.07.2018 06:03	19.07.2018 07:25	54° 11.885	07° 02.063	54° 08.030	06° 54.663	4 streamer	4	5
4013	19.07.2018 07:25	19.07.2018 08:02	54° 07.922	06° 54.218	54° 09.876	06° 52.934	4 streamer	4	5
4014	19.07.2018 08:02	19.07.2018 09:25	54° 10.131	06° 53.267	54° 09.960	07° 03.304	4 streamer	4	5
5001	19.07.2018 15:10	19.07.2018 16:27	54° 11.889	06° 58.101	54° 08.671	06° 57.793	P-cable	3	5
5002	19.07.2018 16:41	19.07.2018 18:00	54° 08.686	06° 58.194	54° 11.979	06° 58.511	P-cable	3	5
5003	19.07.2018 18:19	19.07.2018 19:27	54° 11.853	06° 58.138	54° 08.659	06° 57.838	P-cable	3	5
6001	20.07.2018 11:08	20.07.2018 12:44	54° 06.473	06° 57.929	54° 13.063	06° 58.618	17 streamer	4	5
6002	20.07.2018 13:04	20.07.2018 14:29	54° 12.995	06° 58.450	54° 07.219	06° 57.734	17 streamer	4	5
6003	20.07.2018 14:39	20.07.2018 16:02	54° 07.177	06° 58.327	54° 12.969	06° 58.736	17 streamer	4	5
6005	20.07.2018 18:20	20.07.2018 19:54	54° 09.858	07° 04.024	54° 10.166	06° 53.235	17 streamer	4	5

6006	20.07.2018 20:12	20.07.2018 21:34	54° 09.754	06° 53.750	54° 09.392	07° 02.989	17 streamer	4	5
6007	20.07.2018 21:59	20.07.2018 23:22	54° 10.003	07° 03.051	54° 10.313	06° 53.374	17 streamer	4	5
6008	20.07.2018 23:43	21.07.2018 01:10	54° 10.049	06° 52.998	54° 09.709	07° 03.249	17 streamer	4	5
6009	21.07.2018 01:25	21.07.2018 02:48	54°10.289	07° 03.205	54° 10.606	06° 53.631	17 streamer	4	5
6010	21.07.2018 03:00	21.07.2018 03:50	54° 11.487	06° 53.287	54° 14.992	06° 53.373	17 streamer	4	5
6011	21.07.2018 03:57	21.07.2018 08:07	54° 15.001	06° 53.736	54° 15.003	07° 23.465	17 streamer	4	5
6012	21.07.2018 08:23	21.07.2018 09:19	54° 14.009	07° 23.998	54° 10.128	07° 24.000	17 streamer	4	5
6013	21.07.2018 09:32	21.07.2018 14:05	54° 10.021	07° 22.663	54°10.009	06° 51.372	17 streamer	4	5
6014	21.07.2018 14:14	21.07.2018 15:18	54°10.452	06°51.011	54°14.937	06°50.992	17 streamer	4	5
6015	21.07.2018 15:20	21.07.2018 15:51	54°15.028	06°51.153	54°15.008	06°54.791	17 streamer	4	5
6016	21.07.2018 15:54	21.07.2018 18:14	54°14.886	06°55.038	54° 05.014	06° 54.957	17 streamer	4	5
6017	21.07.2018 18:23	21.07.2018 18:48	54° 04.998	06° 53.960	54° 05.002	06° 51.085	17 streamer	4	5
6018	21.07.2018 18:52	21.07.2018 19:30	54° 05.290	06° 50.996	54° 07.643	06° 50.990	17 streamer	4	5
6019	21.07.2018 19:36	21.07.2018 21:10	54° 08.004	06° 51.534	54° 08.007	07° 02.291	17 streamer	4	5
6020	21.07.2018 21:17	21.07.2018 23:04	54° 08.342	07° 02.488	54°15.545	07° 02.508	17 streamer	4	5
6021	21.07.2018 23:33	22.07.2018 01:45	54° 15.612	07° 59.995	54° 06.667	06° 59.978	17 streamer	4	5
6022	22.07.2018 01:45	22.07.2018 02:43	54° 06.667	06° 59.978	54° 05.841	07° 07.069	17 streamer	4	5

6023	22.07.2018 02:45	22.07.2018 03:11	54° 05.690	07° 07.230	54° 04.206	07° 07.229	17 streamer	4	5
6024	22.07.2018 03:11	22.07.2018 05:40	54° 04.207	07° 07.230	54° 11.997	06° 55.313	17 streamer	4	5
7001	22.07.2018 14:22	22.07.2018 14:47	54° 12.042	07° 04.106			17 streamer	4	5
7002	22.07.2018 14:49	22.07.2018 20:30	54° 13.828	07° 05.035	54° 30.152	07° 34.452	17 streamer	4	5
7003	22.07.2018 20:35	22.07.2018 21:23	54° 30.395	07° 34.305	54° 32.122	07° 29.378	17 streamer	4	5
7004	22.07.2018 21:30	22.07.2018 23:17	54° 31.960	07° 28.773	54° 26.751	07° 19.856	17 streamer	4	5
7005	22.07.2018 23:21	22.07.2018 00:23	54° 26.488	07° 19.781	54° 23.531	07° 25.116	17 streamer	4	5
7006	22.07.2018 00:29	23.07.2018 00:54	54° 23.596	07° 25.667	54° 24.804	07° 27.842	17 streamer	4	5
7007	23.07.2018 00:59	23.07.2018 02:31	54° 25.052	07° 27.886	54° 29.367	07° 19.917	17 streamer	4	5
7008	23.07.2018 02:34	23.07.2018 03:31	54° 29.524	07° 19.843	54° 33.262	07° 22.413	17 streamer	4	5
7009	23.07.2018 03:35	23.07.2018 04:10	54° 33.491	07° 22.335	54° 34.043	07° 18.370	17 streamer	4	5
7010	23.07.2018 04:12	23.07.2018 05:18	54° 33.999	07° 17.954	54° 29.814	07° 16.198	17 streamer	4	5

8 List of Stations

Table 5: Station list of AL512

Station - Device Operation	date time	Device	Action	Latitude	Longitude
AL512_1-2	2018/07/15 15:04:29	Multibeam	in Moonpool	54° 04.989' N	007° 05.929' E
AL512_1-2	2018/07/23 07:37:38	Multibeam	profile start	54° 28.666' N	007° 20.188' E
AL512_1-2	2018/07/23 17:13:52	Multibeam	profile end	54° 26.028' N	007° 25.473' E
AL512_0 Underway-1	2018/07/15 15:12:55	Thermosalinograph	profile start	54° 00.817' N	007° 30.635' E
AL512_1-1	2018/07/15 15:12:55	Seismic Towed Receiver	Streamer in water	54° 02.372' N	007° 09.470' E
AL512_1-1	2018/07/16 06:32:30	Seismic Towed Receiver	Streamer on deck	54° 14.938' N	006° 58.981' E
AL512_0 Underway-1	2018/07/24 05:15:54	Thermosalinograph	profile end	53° 52.911' N	009° 06.084' E
AL512_1-3	2018/07/15 15:34:42	Seismic Source	Airgun in water	54° 06.085' N	007° 04.200' E
AL512_1-3	2018/07/15 16:40:46	Seismic Source	Airgun on deck	54° 09.286' N	006° 59.358' E
AL512_1-3	2018/07/15 17:01:52	Seismic Source	Airgun in water	54° 10.123' N	006° 58.125' E
AL512_1-3	2018/07/16 06:18:38	Seismic Source	Airgun on deck	54° 15.457' N	006° 59.171' E
AL512_1-4	2018/07/15 15:48:15	Seismic Source	profile start	54° 06.683' N	007° 03.348' E
AL512_1-4	2018/07/15 17:02:27	Seismic Source	profile end	54° 10.147' N	006° 58.092' E
AL512_1-4	2018/07/15 18:39:39	Seismic Source	profile start	54° 10.327' N	006° 49.088' E
AL512_1-4	2018/07/15 21:11:08	Seismic Source	profile end	54° 09.701' N	007° 07.317' E
AL512_1-4	2018/07/15 21:16:41	Seismic Source	profile start	54° 09.983' N	007° 07.591' E
AL512_1-4	2018/07/15 22:35:53	Seismic Source	profile end	54° 15.401' N	007° 08.008' E
AL512_1-4	2018/07/15 22:57:01	Seismic Source	profile end	54° 15.302' N	007° 08.030' E
AL512_1-4	2018/07/16 02:32:40	Seismic Source	profile end	54° 04.973' N	006° 48.678' E
AL512_1-4	2018/07/16 02:48:01	Seismic Source	profile start	54° 04.906' N	006° 48.497' E
AL512_1-4	2018/07/16 04:02:09	Seismic Source	profile end	54° 06.297' N	006° 57.315' E
AL512_1-4	2018/07/16 04:06:11	Seismic Source	profile start	54° 06.476' N	006° 57.695' E
AL512_1-4	2018/07/16 06:05:49	Seismic Source	profile end	54° 15.663' N	006° 58.826' E
AL512_2-1	2018/07/16 07:16:07	CTD	in the water	54° 14.930' N	006° 59.199' E
AL512_2-1	2018/07/16 07:20:13	CTD	on deck	54° 14.950' N	006° 59.223' E
AL512_3-1	2018/07/16 08:37:40	Seismic Ocean Bottom Receiver	OBS deployed	54° 10.020' N	006° 58.274' E
AL512_4-1	2018/07/16 08:53:28	Seismic Ocean Bottom Receiver	OBS deployed	54° 10.011' N	006° 58.139' E
AL512_5-1	2018/07/16 09:10:54	Seismic Ocean Bottom Receiver	OBS deployed	54° 10.081' N	006° 58.327' E
AL512_6-1	2018/07/16 10:36:33	Seismic Ocean Bottom Receiver	OBS deployed	54° 10.001' N	006° 58.436' E
AL512_7-1	2018/07/16 10:54:17	Seismic Ocean Bottom Receiver	OBS deployed	54° 09.922' N	006° 58.283' E
AL512_8-1	2018/07/16 11:08:53	Seismic Ocean Bottom Receiver	OBS deployed	54° 10.083' N	006° 57.967' E
AL512_9-1	2018/07/16 12:05:52	Seismic Ocean Bottom Receiver	OBS deployed	54° 10.145' N	006° 58.083' E

AL512_10-1	2018/07/16 12:20:24	Seismic Ocean Bottom Receiver	OBS deployed	54° 10.192' N	006° 58.309' E
AL512_11-1	2018/07/16 12:34:35	Seismic Ocean Bottom Receiver	OBS deployed	54° 10.129' N	006° 58.526' E
AL512_12-1	2018/07/16 13:13:00	Seismic Ocean Bottom Receiver	OBS deployed	54° 09.988' N	006° 58.609' E
AL512_13-1	2018/07/16 13:23:22	Seismic Ocean Bottom Receiver	OBS deployed	54° 09.861' N	006° 58.510' E
AL512_14-1	2018/07/16 13:33:04	Seismic Ocean Bottom Receiver	OBS deployed	54° 09.806' N	006° 58.267' E
AL512_15-1	2018/07/16 14:08:15	Seismic Ocean Bottom Receiver	OBS deployed	54° 09.876' N	006° 58.053' E
AL512_16-1	2018/07/16 14:21:06	Seismic Ocean Bottom Receiver	OBS deployed	54° 10.413' N	006° 58.307' E
AL512_17-1	2018/07/16 14:38:17	Seismic Ocean Bottom Receiver	OBS deployed	54° 09.607' N	006° 58.228' E
AL512_18-1	2018/07/16 14:51:26	CTD	in the water	54° 09.590' N	006° 58.292' E
AL512_18-1	2018/07/16 14:56:30	CTD	on deck	54° 09.587' N	006° 58.289' E
AL512_19-1	2018/07/16 17:06:46	Multibeam	profile start	54° 09.013' N	006° 59.935' E
AL512_19-1	2018/07/17 05:01:00	Multibeam	profile end	54° 10.749' N	006° 55.876' E
AL512_20-1	2018/07/16 19:15:56	CTD	in the water	54° 09.334' N	006° 59.076' E
AL512_20-1	2018/07/16 19:17:40	CTD	on deck	54° 09.341' N	006° 59.314' E
AL512_21-1	2018/07/17 00:10:37	CTD	in the water	54° 10.011' N	006° 58.287' E
AL512_21-1	2018/07/17 00:13:07	CTD	on deck	54° 10.017' N	006° 58.287' E
AL512_22-1	2018/07/17 03:19:26	CTD	in the water	54° 10.462' N	006° 59.937' E
AL512_22-1	2018/07/17 03:22:09	CTD	on deck	54° 10.455' N	006° 59.921' E
AL512_23-1	2018/07/17 07:33:00	Seismic Towed Receiver	PCable in water	54° 11.082' N	007° 08.946' E
AL512_23-1	2018/07/17 12:44:42	Seismic Towed Receiver	PCable on deck	54° 14.073' N	006° 51.320' E
AL512_23-2	2018/07/17 09:11:31	Seismic Source	Airgun in water	54° 11.480' N	007° 04.326' E
AL512_23-2	2018/07/17 09:55:49	Seismic Source	on deck	54° 12.043' N	007° 00.873' E
AL512_24-1	2018/07/17 14:47:57	Multibeam	profile start	54° 09.901' N	006° 55.655' E
AL512_24-1	2018/07/17 16:22:47	Multibeam	profile end	54° 09.865' N	006° 55.543' E
AL512_25-1	2018/07/17 17:07:19	Fish Finder Echosounder	profile start	54° 09.992' N	006° 58.262' E
AL512_25-1	2018/07/18 05:04:10	Fish Finder Echosounder	profile end	54° 09.872' N	006° 58.354' E
AL512_26-1	2018/07/18 06:10:34	Seismic Source	Airgun in water	54° 10.288' N	007° 03.748' E
AL512_26-1	2018/07/18 07:02:00	Seismic Source	profile start	54° 09.966' N	006° 58.876' E
AL512_26-1	2018/07/18 11:18:44	Seismic Source	profile end	54° 06.753' N	006° 57.956' E
AL512_26-1	2018/07/18 11:56:30	Seismic Source	Airgun on deck	54° 06.885' N	006° 55.656' E
AL512_26-1	2018/07/18 12:09:25	Seismic Source	Airgun in water	54° 06.961' N	006° 54.912' E
AL512_26-1	2018/07/19 10:02:15	Seismic Source	Airgun on deck	54° 10.353' N	007° 07.693' E
AL512_26-2	2018/07/18 12:21:35	Seismic Towed Receiver	Streamer in water	54° 07.024' N	006° 54.245' E
AL512_26-2	2018/07/18 14:12:19	Seismic Towed Receiver	profile start	54° 07.677' N	007° 01.446' E
AL512_26-2	2018/07/18 15:34:59	Seismic Towed Receiver	profile end	54° 11.980' N	006° 54.967' E
AL512_26-2	2018/07/18 15:42:56	Seismic Towed Receiver	profile start	54° 12.169' N	006° 54.931' E

AL512_26-2	2018/07/18 17:07:18	Seismic Towed Receiver	profile end	54° 07.913' N	007° 01.449' E
AL512_26-2	2018/07/18 17:14:38	Seismic Towed Receiver	profile start	54° 07.913' N	007° 01.755' E
AL512_26-2	2018/07/18 18:37:01	Seismic Towed Receiver	profile end	54° 12.238' N	006° 55.191' E
AL512_26-2	2018/07/18 18:48:12	Seismic Towed Receiver	profile start	54° 12.146' N	006° 54.891' E
AL512_26-2	2018/07/18 20:10:10	Seismic Towed Receiver	profile end	54° 07.852' N	007° 01.414' E
AL512_26-2	2018/07/18 20:19:54	Seismic Towed Receiver	profile start	54° 07.905' N	007° 01.610' E
AL512_26-2	2018/07/18 21:41:31	Seismic Towed Receiver	profile end	54° 12.220' N	006° 55.040' E
AL512_26-2	2018/07/18 22:52:18	Seismic Towed Receiver	profile start	54° 12.007' N	007° 01.863' E
AL512_26-2	2018/07/19 00:19:07	Seismic Towed Receiver	profile end	54° 08.195' N	006° 54.505' E
AL512_26-2	2018/07/19 00:29:41	Seismic Towed Receiver	profile start	54° 08.089' N	006° 54.700' E
AL512_26-2	2018/07/19 01:27:23	Seismic Towed Receiver	profile end	54° 10.820' N	006° 59.875' E
AL512_26-2	2018/07/19 02:01:43	Seismic Towed Receiver	profile start	54° 10.360' N	006° 58.952' E
AL512_26-2	2018/07/19 02:34:24	Seismic Towed Receiver	profile end	54° 11.901' N	007° 01.885' E
AL512_26-2	2018/07/19 02:43:22	Seismic Towed Receiver	profile start	54° 11.879' N	007° 02.232' E
AL512_26-2	2018/07/19 03:58:08	Seismic Towed Receiver	profile end	54° 08.394' N	006° 55.548' E
AL512_26-2	2018/07/19 05:54:29	Seismic Towed Receiver	profile end	54° 11.915' N	007° 01.790' E
AL512_26-2	2018/07/19 06:03:33	Seismic Towed Receiver	profile start	54° 11.893' N	007° 02.077' E
AL512_26-2	2018/07/19 07:25:39	Seismic Towed Receiver	profile end	54° 08.044' N	006° 54.688' E
AL512_26-2	2018/07/19 08:04:03	Seismic Towed Receiver	profile start	54° 10.128' N	006° 53.457' E
AL512_26-2	2018/07/19 09:24:54	Seismic Towed Receiver	profile end	54° 09.961' N	007° 03.279' E
AL512_26-2	2018/07/19 10:12:39	Seismic Towed Receiver	Streamer on deck	54° 10.453' N	007° 08.453' E
AL512_27-1	2018/07/19 11:45:12	Seismic Towed Receiver	PCable in water	54° 13.296' N	007° 08.162' E
AL512_27-1	2018/07/19 15:10:13	Seismic Towed Receiver	profile start	54° 11.911' N	006° 58.107' E
AL512_27-1	2018/07/19 16:26:35	Seismic Towed Receiver	profile end	54° 08.675' N	006° 57.793' E
AL512_27-1	2018/07/19 16:41:31	Seismic Towed Receiver	profile start	54° 08.676' N	006° 58.192' E
AL512_27-1	2018/07/19 18:00:23	Seismic Towed Receiver	profile end	54° 11.996' N	006° 58.519' E
AL512_27-1	2018/07/19 20:29:11	Seismic Towed Receiver	PCable on deck	54° 09.679' N	006° 57.944' E
AL512_27-2	2018/07/19 13:13:11	Seismic Source	Airgun in water	54° 13.315' N	007° 04.360' E

AL512_27-2	2018/07/19 18:20:06	Seismic Source	profile start	54° 11.826' N	006° 58.141' E
AL512_27-2	2018/07/19 19:27:45	Seismic Source	profile end	54° 08.670' N	006° 57.837' E
AL512_27-2	2018/07/19 19:38:38	Seismic Source	Airgun on deck	54° 08.686' N	006° 57.984' E
AL512_28-1	2018/07/19 21:23:19	CTD	in the water	54° 10.275' N	006° 55.687' E
AL512_28-1	2018/07/19 21:27:17	CTD	on deck	54° 10.312' N	006° 55.621' E
AL512_29-1	2018/07/19 21:34:30	Multibeam	profile start	54° 10.356' N	006° 55.939' E
AL512_29-1	2018/07/20 05:13:30	Multibeam	profile end	54° 09.280' N	006° 56.066' E
AL512_30-1	2018/07/20 03:15:17	CTD	in the water	54° 09.741' N	006° 59.944' E
AL512_30-1	2018/07/20 03:19:31	CTD	on deck	54° 09.749' N	006° 59.930' E
AL512_31-1	2018/07/20 05:46:55	Multibeam	profile start	54° 09.733' N	006° 58.220' E
AL512_31-1	2018/07/20 09:08:26	Multibeam	profile end	54° 10.131' N	006° 58.551' E
AL512_32-1	2018/07/20 09:19:52	CTD	in the water	54° 09.948' N	006° 58.175' E
AL512_32-1	2018/07/20 09:23:47	CTD	on deck	54° 09.966' N	006° 58.183' E
AL512_33-1	2018/07/20 10:24:27	Seismic Towed Receiver	Streamer in water	54° 06.077' N	006° 55.272' E
AL512_33-1	2018/07/22 06:17:13	Seismic Towed Receiver	Streamer on deck	54° 11.050' N	006° 57.628' E
AL512_33-2	2018/07/20 10:31:32	Seismic Source	Airgun in water	54° 06.062' N	006° 55.669' E
AL512_33-2	2018/07/20 11:08:41	Seismic Source	profile start	54° 06.510' N	006° 57.931' E
AL512_33-2	2018/07/20 12:45:25	Seismic Source	profile end	54° 13.093' N	006° 58.622' E
AL512_33-2	2018/07/20 13:07:13	Seismic Source	profile start	54° 12.834' N	006° 58.389' E
AL512_33-2	2018/07/20 14:28:54	Seismic Source	profile end	54° 07.254' N	006° 57.739' E
AL512_33-2	2018/07/20 14:39:23	Seismic Source	profile start	54° 07.182' N	006° 58.326' E
AL512_33-2	2018/07/20 16:02:14	Seismic Source	profile end	54° 12.871' N	006° 58.708' E
AL512_33-2	2018/07/20 16:57:23	Seismic Source	Airgun on deck	54° 11.220' N	007° 03.681' E
AL512_33-2	2018/07/20 17:56:47	Seismic Source	Airgun in water	54° 10.305' N	007° 06.658' E
AL512_33-2	2018/07/20 17:59:06	Seismic Source	profile start	54° 10.247' N	007° 06.431' E
AL512_33-2	2018/07/21 02:48:04	Seismic Source	profile end	54° 10.606' N	006° 53.639' E
AL512_34-1	2018/07/21 03:53:26	Seismic Source	profile start	54° 15.004' N	006° 53.764' E
AL512_34-1	2018/07/22 01:45:21	Seismic Source	profile end	54° 06.698' N	006° 59.976' E
AL512_35-1	2018/07/22 03:13:59	Seismic Towed Receiver	profile start	54° 04.298' N	007° 06.953' E
AL512_35-1	2018/07/22 05:36:39	Seismic Towed Receiver	profile end	54° 11.786' N	006° 55.631' E
AL512_35-1	2018/07/22 06:16:26	Seismic Towed Receiver	Streamer on deck	54° 11.070' N	006° 57.579' E
AL512_36-1	2018/07/22 06:38:31	Seismic Ocean Bottom Receiver	released	54° 09.968' N	006° 58.453' E
AL512_36-1	2018/07/22 06:49:10	Seismic Ocean Bottom Receiver	on deck	54° 09.998' N	006° 58.334' E
AL512_37-1	2018/07/22 06:52:48	Seismic Ocean Bottom Receiver	released	54° 09.964' N	006° 58.366' E
AL512_37-1	2018/07/22 06:58:55	Seismic Ocean Bottom Receiver	on deck	54° 09.986' N	006° 58.108' E
AL512_38-1	2018/07/22 07:07:27	Seismic Ocean Bottom Receiver	released	54° 10.043' N	006° 58.485' E
AL512_38-1	2018/07/22 07:12:30	Seismic Ocean Bottom Receiver	on deck	54° 10.099' N	006° 58.321' E
AL512_39-1	2018/07/22 07:19:45	Seismic Ocean Bottom Receiver	released	54° 09.934' N	006° 58.654' E

AL512_39-1	2018/07/22 07:25:40	Seismic Ocean Bottom Receiver	on deck	54° 10.070' N	006° 58.359' E
AL512_40-1	2018/07/22 07:33:45	Seismic Ocean Bottom Receiver	released	54° 09.843' N	006° 58.414' E
AL512_40-1	2018/07/22 07:39:21	Seismic Ocean Bottom Receiver	on deck	54° 09.931' N	006° 58.276' E
AL512_41-1	2018/07/22 07:41:11	Seismic Ocean Bottom Receiver	released	54° 09.953' N	006° 58.242' E
AL512_41-1	2018/07/22 07:52:53	Seismic Ocean Bottom Receiver	on deck	54° 10.067' N	006° 57.951' E
AL512_42-1	2018/07/22 07:57:53	Seismic Ocean Bottom Receiver	released	54° 10.018' N	006° 58.018' E
AL512_42-1	2018/07/22 08:03:16	Seismic Ocean Bottom Receiver	on deck	54° 10.165' N	006° 58.078' E
AL512_43-1	2018/07/22 08:05:58	Seismic Ocean Bottom Receiver	released	54° 10.202' N	006° 58.089' E
AL512_43-1	2018/07/22 08:11:18	Seismic Ocean Bottom Receiver	on deck	54° 10.187' N	006° 58.343' E
AL512_44-1	2018/07/22 08:13:10	Seismic Ocean Bottom Receiver	released	54° 10.184' N	006° 58.362' E
AL512_44-1	2018/07/22 08:19:13	Seismic Ocean Bottom Receiver	on deck	54° 10.141' N	006° 58.508' E
AL512_45-1	2018/07/22 08:21:43	Seismic Ocean Bottom Receiver	released	54° 10.140' N	006° 58.526' E
AL512_45-1	2018/07/22 08:28:37	Seismic Ocean Bottom Receiver	on deck	54° 10.002' N	006° 58.579' E
AL512_46-1	2018/07/22 08:30:58	Seismic Ocean Bottom Receiver	released	54° 09.996' N	006° 58.600' E
AL512_46-1	2018/07/22 08:37:30	Seismic Ocean Bottom Receiver	on deck	54° 09.860' N	006° 58.427' E
AL512_47-1	2018/07/22 08:39:06	Seismic Ocean Bottom Receiver	released	54° 09.857' N	006° 58.400' E
AL512_47-1	2018/07/22 08:45:11	Seismic Ocean Bottom Receiver	on deck	54° 09.810' N	006° 58.185' E
AL512_48-1	2018/07/22 08:46:39	Seismic Ocean Bottom Receiver	released	54° 09.810' N	006° 58.157' E
AL512_48-1	2018/07/22 08:52:17	Seismic Ocean Bottom Receiver	on deck	54° 09.874' N	006° 57.936' E
AL512_49-1	2018/07/22 09:01:55	Seismic Ocean Bottom Receiver	released	54° 09.689' N	006° 58.047' E
AL512_49-1	2018/07/22 09:07:05	Seismic Ocean Bottom Receiver	on deck	54° 09.602' N	006° 58.150' E
AL512_50-1	2018/07/22 09:18:51	Seismic Ocean Bottom Receiver	released	54° 10.263' N	006° 58.133' E
AL512_50-1	2018/07/22 09:25:42	Seismic Ocean Bottom Receiver	on deck	54° 10.420' N	006° 58.194' E
AL512_51-1	2018/07/22 10:20:39	Grab	in the water	54° 10.080' N	006° 58.272' E
AL512_51-1	2018/07/22 10:23:11	Grab	on deck	54° 10.077' N	006° 58.266' E
AL512_52-1	2018/07/22 10:47:53	Grab	in the water	54° 09.891' N	006° 58.307' E
AL512_52-1	2018/07/22 10:50:20	Grab	on deck	54° 09.897' N	006° 58.292' E
AL512_53-1	2018/07/22 10:58:23	Grab	in the water	54° 09.877' N	006° 58.298' E
AL512_53-1	2018/07/22 11:00:16	Grab	on deck	54° 09.879' N	006° 58.296' E
AL512_54-1	2018/07/22 11:14:26	Grab	in the water	54° 10.013' N	006° 58.289' E
AL512_54-1	2018/07/22 11:16:35	Grab	on deck	54° 10.010' N	006° 58.289' E

AL512_55-1	2018/07/22 11:36:18	Grab	in the water	54° 10.019' N	006° 58.164' E
AL512_55-1	2018/07/22 11:38:27	Grab	on deck	54° 10.015' N	006° 58.164' E
AL512_56-1	2018/07/22 11:59:02	Grab	in the water	54° 10.023' N	006° 58.101' E
AL512_56-1	2018/07/22 12:02:02	Grab	on deck	54° 10.026' N	006° 58.074' E
AL512_57-1	2018/07/22 12:17:59	Grab	in the water	54° 10.027' N	006° 58.002' E
AL512_57-1	2018/07/22 12:21:04	Grab	on deck	54° 10.024' N	006° 57.986' E
AL512_58-1	2018/07/22 12:37:32	Grab	in the water	54° 10.012' N	006° 58.379' E
AL512_58-1	2018/07/22 12:40:54	Grab	on deck	54° 10.008' N	006° 58.400' E
AL512_59-1	2018/07/22 13:28:06	Grab	in the water	54° 09.851' N	007° 02.738' E
AL512_59-1	2018/07/22 13:30:30	Grab	on deck	54° 09.853' N	007° 02.739' E
AL512_60-1	2018/07/22 13:52:27	Seismic Towed Receiver	Streamer in water	54° 10.187' N	007° 03.374' E
AL512_60-1	2018/07/22 14:15:56	Seismic Towed Receiver	profile start	54° 11.572' N	007° 03.919' E
AL512_60-1	2018/07/23 05:18:18	Seismic Towed Receiver	profile end	54° 29.843' N	007° 16.212' E
AL512_60-1	2018/07/23 06:04:08	Seismic Towed Receiver	on deck	54° 29.855' N	007° 13.725' E
AL512_60-2	2018/07/22 13:55:58	Seismic Source	Airgun in water	54° 10.360' N	007° 03.431' E
AL512_60-2	2018/07/23 05:58:48	Seismic Source	on deck	54° 29.839' N	007° 13.885' E
AL512_61-1	2018/07/23 06:10:32	CTD	in the water	54° 29.850' N	007° 13.619' E
AL512_61-1	2018/07/23 06:16:18	CTD	on deck	54° 29.829' N	007° 13.645' E
AL512_62-1	2018/07/23 12:18:40	CTD	in the water	54° 28.963' N	007° 20.185' E
AL512_62-1	2018/07/23 12:25:02	CTD	on deck	54° 28.581' N	007° 20.602' E
AL512_63-1	2018/07/23 14:19:28	CTD	in the water	54° 28.984' N	007° 20.546' E
AL512_63-1	2018/07/23 14:21:57	CTD	on deck	54° 28.995' N	007° 20.539' E
AL512_64-1	2018/07/23 17:17:28	CTD	in the water	54° 25.887' N	007° 25.625' E
AL512_64-1	2018/07/23 17:20:24	CTD	on deck	54° 25.861' N	007° 25.623' E
AL512_65-1	2018/07/23 17:20:30	Multibeam	in Moonpool	54° 25.860' N	007° 25.624' E
AL512_65-1	2018/07/23 18:47:10	Multibeam	out Moonpool	54° 26.567' N	007° 24.723' E